This is the post-print version of the following article: *Marta Quintanilla, Malou Henriksen-Lacey, Carlos Renero-Lecuna, and Luis M. Liz-Marzán, Challenges for optical nanothermometry in biological environments, Chemical Society Reviews, 2022*, 51, 4223-4242

DOI: 10.1039/D2CS00069E

Challenges for optical nanothermometry in biological environments

Marta Quintanilla,[1*] Malou Henriksen-Lacey,[2,3] Carlos Renero-Lecuna,[2,3] and Luis M. Liz-Marzán[2,3,4*]

[1]Materials Physics Department, Universidad Autónoma de Madrid (UAM). Avda. Francisco Tomás y Valiente, 7. 28049, Madrid, Spain
[2]CIC biomaGUNE, Basque Research and Technology Alliance (BRTA). Paseo de Miramón 194, 20014 Donostia-San Sebastián, Spain
[3]Centro de Investigación Biomédica en Red, Bioingeniería, Biomateriales y Nanomedicina (CIBER-BBN), Paseo de Miramón 194, 20014 Donostia-San Sebastián, Spain
[4]Ikerbasque, Basque Foundation for Science, 48009 Bilbao, Spain

*Corresponding authors' emails: marta.quintanilla@uam.es (M.Q.); llizmarzan@cicbiomagune.es (L.M.L.-M.)

ABSTRACT Temperature monitoring is useful in medical diagnosis, and essential during hyperthermia treatments to avoid undesired cytotoxic effects. Aiming to control heating doses, different temperature monitoring strategies have been developed, largely based on luminescent materials, a.k.a. nanothermometers. However, for such nanothermometers to work, both excitation and emission light beams must travel through tissue, making its optical properties a relevant aspect to be considered during the measurements. In complex tissues, heterogeneity, and real-time alterations as a result of therapeutic treatment may have an effect on light-tissue interaction, hindering accuracy in the thermal reading. In this Tutorial Review we discuss various methods in which nanothermometers can be used for temperature sensing within heterogeneous environments. We discuss recent developments in optical (nano)thermometry, focusing on the incorporation of luminescent nanoparticles into complex *in vitro* and *in vivo* models. Methods formulated to avoid thermal misreading are also discussed, considering their respective advantages and drawbacks.

KEY LEARNING POINTS
1. Basic principles of luminescence nanothermometry.
2. Nanothermometry applied to biological systems.
3. Insights on tissue effects: thermal reading through non-transparent media.
4. Accuracy of spectroscopy-based temperature measurements in complex models.
5. Outlook and perspectives on luminescent nanomaterials for temperature measurements.

Introduction

The concept of hyperthermia for the treatment of disease has been reported to exist for over 5000 years.[1] Like many other historical medical treatments, with the arrival of modern medicine it became clear that applying and monitoring temperature changes would need careful refinement. Throughout the 20th century, methods to direct heat to internal organs were initially achieved via insertable probes at the site of application.[2] With the development of nanotechnology, new techniques have been proposed to achieve localized hyperthermia, based on the ability of some nanomaterials to transform magnetic fields or light into heat. Indeed, some formulations of nanomaterials are currently (January, 2022) at different stages of clinical trials, targeting prostate, lung or head and neck cancers. However, optimal treatment not only requires spatial control of the heated area, but also on the achieved temperature, to avoid overexposure and damage of the surrounding tissue. In clinical settings, current recommendations to implement thermally monitored hyperthermia are mainly related to the treatment of liver cancer. Hyperthermia is also of interest in different experimental settings, for applications such as rewarming of cryopreserved organs, activation of thermo-sensitive properties in materials science, ablation of cancer cells in oncology studies via specific delivery of strongly absorbing nanoparticles, etc.

Thermal monitoring alone also plays an important role in the diagnosis of disease state or infections. For example, the early-stage detection of ischemia, thanks to the so-called Transient Thermometry (TTh) technique, or of breast cancer thanks to a higher local temperature promoted by increased metabolic and vascular changes of the tumor.[3,4] Changes in temperature, whether they are internally or externally provoked, can thus be exploited for both the diagnosis and treatment of many diseases. Notwithstanding, the vast array of tissue heterogeneity as well as the differences in the temperature ranges of interest over space and time for different applications, imply that there is no "one size fits all" rule for thermometry requirements. However, certain requisites such as non-invasiveness, accuracy, and sensitivity are all generally shared among clinical applications.

When the focus is on measuring temperature at *in vitro* and *in vivo* settings with an ultimate clinical target, an aspect that has not been sufficiently addressed is its accurate determination in real-time with high spatial resolution. Opposite to traditional contact probes, such as liquid-in-glass thermometers, thermocouples or optical fibres, purely non-contact techniques based on spectroscopy have been developed toward this aim. However, commercially available tools (e.g., infrared (IR) thermal cameras) have limited sensitivity and accuracy, and whilst non-invasive, their ability to detect temperature changes is restricted to surface measurements, due to the poor tissue penetration of mid-far IR light, where these cameras are designed to

operate (typically from 6 to 14 μm). Indeed, there are strong limitations regarding working wavelengths that not only affect the maximum depth of the measurement, but also the accuracy of the technique, both *in vitro* and *in vivo*. Organs comprising different tissues present strong scattering of light because of the various physical interfaces at tissue boundaries.[5] Furthermore, large signal distortions take place in photoluminescence spectra when such interfaces are combined with highly absorbing molecules such as haemoglobin and lipids. To overcome these issues, thermal measurements are generally based on detection mechanisms in the near infrared (NIR) range of the electromagnetic spectrum, which is optimal for biomedical thermography. To date, up to four spectral ranges, also known as "Biological Windows" (BWs), in which both light scattering and absorption from molecules are reduced, have been identified within the NIR. Their exact widths vary depending on the publication in question, but approximate ranges can be identified as 650 - 950 nm (BW-I), 1000 - 1350 nm (BW-II), 1450 - 1900 nm (BW-III), and 2100 - 2300 nm (BW-IV).[6,7] Various non-contact thermometry techniques can be adapted to work within these BWs, for example Raman spectroscopy and interferometry thermography. Whereas the former relies on the detection of vibrational modes in the material, the latter deduces temperature values from changes in the refractive index of the sample. Yet, given the heterogeneous nature of biological environments, which include a multitude of biocomponents with huge variations in refractive indexes, the interpretation of these techniques can be very complex. As an alternative to purely non-invasive spectroscopy and the traditional contact probes, an additional category of thermometry sensors have emerged: luminescent nanomaterials (LNMs).

We define LNMs as nanoparticles and other nanomaterials such as polymers, nanoclusters, etc., that can be used as thermometers because their luminescence is sensitive to temperature changes. Compared to other temperature sensing techniques, the use of LNMs is generally non-invasive because their luminescence can be excited from sources external to the sample. Additionally, their nanoscale size translates into a relatively high spatial resolution, which in the absence of scattering from tissue, is typically limited by light diffraction. This nanometric scale also facilitates delivery to a wide range of target organelles, cells, tissues and organs. As opposed to IR cameras, LNMs offer the possibility to detect temperature changes at internal sites, and luminescence offers in principle an easier way to calculate the temperature, as compared to other spectroscopy techniques. As a result, such materials can potentially be used in a variety of therapeutic and diagnostic applications involving internal organs.

The use of LNM temperature measurements was first described in the 1970's, but it was not until the last decade that they were employed in biological research. During this period, outstanding progress in the synthesis and characterization of LNMs took place, and whereas the initial efforts were directed towards exploring new nanomaterials, further advances were focused on tuning the emission and excitation wavelengths to the (farther) biological windows, hence improving light penetration. Besides, the field has necessarily grown in parallel with bionanotechnology, including thus concerns on cell internalization, cytotoxicity, and controlled delivery. One of the characteristics that provide versatility to LNM measurements is the large library of available nanoscale materials, the most commonly described LNMs including organic molecules, quantum dots (or other semiconductor nanoparticles), lanthanide-doped nanoparticles, and nanodiamonds.[7-9] The correct selection of nanothermometers, taking into special consideration the available biological windows, has been described in an excellent review by Nexha et al.[7] In this work it becomes apparent that, whereas abundant literature is available on the synthesis of LNMs, their application to *in vitro* and *in vivo* studies is relatively underexplored.

If we ask ourselves why this is the case, the insufficient choice of nanothermometers cannot be the reason, even though a better signal-to-noise ratio would always facilitate sensing and this remains an important drawback of some materials. Instead, what if a poor understanding of the physicochemical properties of LNMs in biological environments were the cause? Or the lack of technological instrumentation and reproducibility for their accurate detection? Indeed, the latest developments in the field of LNMs are directed towards standardization of the probes, and to the development and implementation of measurement protocols to improve accuracy.

In this Tutorial Review, we aim at describing the importance of LNMs for localized nanothermometry, focusing on the experimental conditions to be considered. This analysis includes the description of the biological environment, which determines light penetration and exit, but also the selection of suitable temperature sensing methods. Materials for nanothermometry have been extensively described in recent reviews,[8,10,11] thus, here we describe the pros and cons concerning their performance in heterogeneous environments. We pay special attention to the obstacles that may arise during temperature measurements, and to the solutions that have been proposed. These are key aspects for the current evolution of nanothermometry, as a poor or incomplete analysis will not only result in poor thermometric performance and thus inaccurate temperature measurements, but additionally can cause undesired tissue damage, unforeseen cytotoxicity, cellular changes at a molecular level, or even instability of NPs, all of which should be avoided in any biological situation.

Relevant Parameters in Luminescence Nanothermometry

Luminescent materials can be used as thermal probes, provided that the light they emit is dependent on temperature in any respect. Indeed, different characteristics of emitted light can be (and have been) exploited to measure temperature (or temperature changes). These parameters include emission intensity and lifetime, spectral width, and spectral shift, as well as intensity ratios and polarization anisotropy (**Figure 1**). The physical processes behind each thermometry technique play a key role in the feasibility of the measurement. First of all, thermal sensitivity, i.e. the

extent of change of the measured parameter per degree, is determined by the physics of luminescence. Second, practical implementation of each specific experimental set-up will affect the cost, speed, and ease of data analysis of the technique. Finally, both nanomaterials and emitted photons will inevitably interact with their environment, resulting in alterations of the detected signal, with various degrees of relevance depending on the physical origin of the measured parameter. Let us briefly discuss the main available options.

The emission probability of an excited fluorophore, i.e., a fluorophore that has absorbed sufficient energy to promote an electron from the ground state to an excited state, is given by the radiative decay rate, k_r. In the same way, there is a non-radiative decay rate, k_{nr}, which is the probability for the fluorophore to transfer its extra energy to the vibrational modes of surrounding atoms or molecules. Let us assume the simple case in which the fluorophore is located in a homogeneous medium, as would be the case for one luminescent dopant in a perfect transparent crystal matrix. Then, k_r and k_{nr} are the only possible relaxation routes and thus, there is a competition between them. While k_r is a constant for a specific dopant-host pair, k_{nr} varies with temperature, which means that the observed emission intensity will also vary with temperature, thereby allowing for thermometry applications. This can be easily seen through the definition of photoluminescence quantum yield, η, which is the ratio between the number of emitted photons and absorbed photons:

$$\eta = \frac{k_r}{k_r + k_{nr}} \quad (1)$$

The other parameter directly related to k_r and k_{nr} that can be used in thermometry is experimental lifetime, τ_{exp}, which measures the characteristic time an electron remains in an excited state before relaxation:

$$\tau_{exp} = \frac{1}{k_r + k_{nr}} \quad (2)$$

Most nanothermometry methods are based on either emission intensity or lifetime measurements, both of which are strongly dependent on temperature and are thus highly sensitive. Changes to the band width and wavelength shifts are less commonly exploited, as the temperature dependent effect is generally weaker and hence less sensitive. Nevertheless, the use of materials such as $Y_2O_3:Eu^{3+}$ nanoparticles with a strongly temperature-dependent bandwidth,[12] Ag_2S nanoparticles featuring emission peak redshifts at higher temperatures,[13] or nanodiamonds in which the energy separation between two energy levels is used as a thermal probe, have been reported.[14] The latter case is interesting as it has provided accurate results including the study of plasmonic heating and *in vitro* temperature reading.[14] However, visible light excitation and microwave pulses are required, which hinders their applicability *in vivo*. All such alternative options are also interesting in the context of the current trend to apply multiparametric analysis based on the thermal dependence of more than one luminescence parameter.[15] This strategy gives access to improved thermal resolution, reaching values as low as 0.05 K, so even if one technique alone cannot reach such a high resolution by itself,

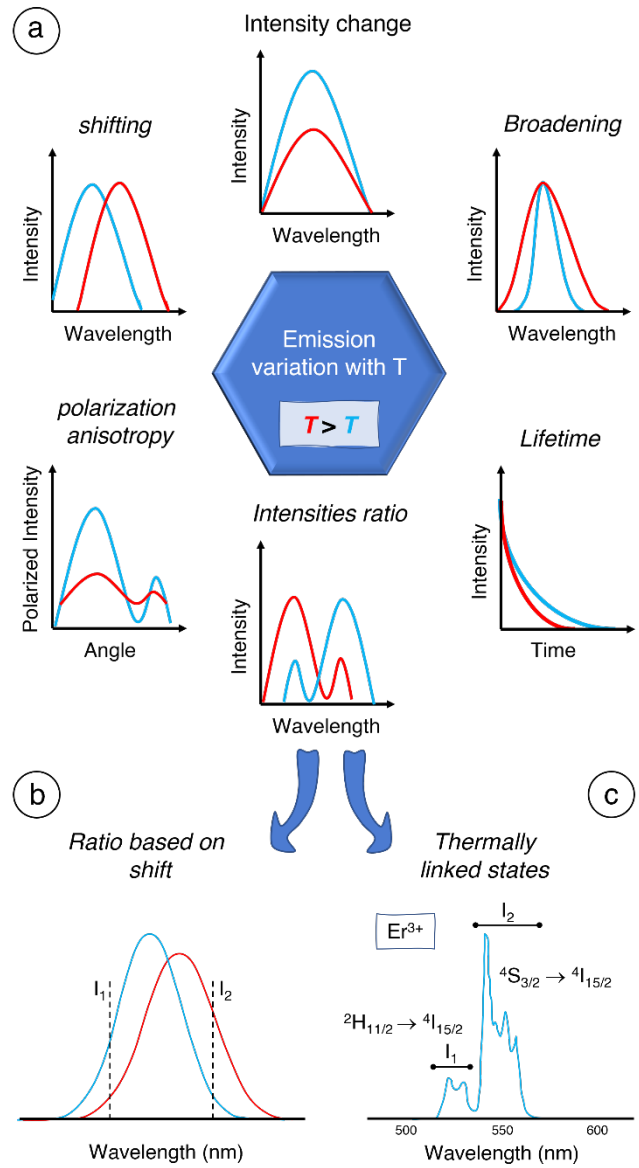

Figure 1. (a) Luminescence-based strategies applied to measure temperature with NPs. (b,c) Intensity ratios have been used in two modalities: to characterize an emission shift (b), or to characterize the emission from two thermalized energy states (c).

a chance arises if complemented with other thermometer probes.

An important advantage of intensity-based thermometry is the simplicity of the experimental set-up and of data processing. Indeed, if the experiment is properly controlled, an accurate thermal calibration allows for a direct correlation between intensity and temperature. The same reason can however also become a limiting factor, as an accurate agreement between calibration and experimental conditions is required. In other words, excitation and emission light beams must reach the nanoparticles and the detector, respectively, in the purest form for temperature to be determined. This factor complicates temperature measurements in heterogenous biological environments where light scattering and absorption may become dominant. In addition, the concentration of LNMs must remain constant and known, as more LNMs will obviously

provide a higher emission intensity. This is a major limitation for *in vivo* situations, as neither the initial density of LNMs in the tissue, nor its variations over time can be easily controlled.

A solution to these drawbacks has been found by measuring the intensity of light at two different wavelengths and using their ratio as a thermometry probe. In this technique, one intensity can be understood as a reference value or internal calibration for the other. Therefore, for the highest thermal sensitivity it is crucial that their intensity variations due to temperature changes are as dissimilar as possible. If both selected intensities show the same dependence on LNM concentration and on excitation power, then the intensity ratio will not be affected by these parameters. These restrictions mean that not every intensity ratio is valid, especially if coming from two separate fluorophores that may not be colocalized, or if non-linear excitation occurs (as in upconversion techniques), as this can trigger different dependencies between emission intensity and excitation power. In general, there are two main situations related to the emission of one single fluorophore in which intensity ratio thermometry has been safely applied.

The first one involves a shift of the emission spectrum when temperature changes (**Figure 1b**). Instead of measuring the emission peak position, it is then possible to simplify data recording by defining an intensity ratio between two different wavelengths within the same emission band. Such a ratio would also be affected by any intensity changes of the emission, which typically occur simultaneously to the shift, so both effects are included in one single parameter. A good example of the use of intensity ratios in such a case is provided by Ag_2S semiconductor nanoparticles, which typically feature one emission band within the second biological window, which shifts and loses intensity as temperature increases.[13] It has been reported that, in this strategy, the accuracy and sensitivity of the intensity ratio depends on a careful selection of the two wavelengths at which emission intensity is to be monitored.

The second situation in which intensity ratios are applied is related to emission bands with contributions from two different excited states (**Figure 1c**). If both energy states are close enough, i.e., typically with a separation smaller than ≈ 2000 cm^{-1}, thermal energy (given by $k_B \cdot T$, $k_B \approx 0.695$ cm^{-1}/K) may be sufficient to promote electrons from the lower energy state to the upper one. Thus, the electronic population of both levels will be thermally linked, and their intensities will constitute a reliable intensity ratio. Most materials displaying this type of energy states are lanthanide-doped nanoparticles. Notwithstanding, some transition metal doped nanoparticles have also been recently reported to display all the required characteristics for this technique.[16] In the case of lanthanides, emission bands are sufficiently narrow so that nearby emission bands can be spectrally resolved and subsequently used for nanothermometry, as shown for I_1 and I_2 in Figure 1c. This is because 4*f* electrons, responsible for luminescence in these materials, are partially shielded from the electromagnetic field created by the surrounding material, which is known as the crystal field. Furthermore, although the effect of the external crystal field is weak, it can break the degeneracy of the energy states in sub-levels separated by only 10^2 cm^{-1}. In the emission spectrum, this translates into a sub-structure of peaks within each emission band (**Figure 1c**, see peaks in each of the two main transitions) that will be close enough to being also thermally linked. In this case, however, the levels are often too close together to be spectrally resolved in measurements, but otherwise could also constitute a thermal probe. Examples of intensity ratios based on thermally linked states are found in most thermometers based on emissions from erbium, in the green spectral region (500 nm – 560 nm), as shown in **Figure 1c**. Shifting towards the NIR, neodymium ions have been also described to display similar properties, with emissions located both in the BW-I (*ca*. 800 nm) and in the BW-II (*ca.* 1050 nm).[8]

The use of intensity ratios is, in principle, a robust strategy to address the issues caused by fluctuations in LNM concentration and excitation power. However, as it is based on luminescence from lanthanide ions, a detection set-up with high spectral resolution and sensitivity is required. This second feature is related to the fact that electronic transitions between 4*f* states are forbidden by selection rules, and thus only emit because an asymmetric crystal (or molecular) field can relax this situation. Still, their absorption cross-sections and emission quantum yields are often lower than those of other luminescent materials, such as quantum dots or fluorescent organic dyes. The need for high spectral resolution is due to the narrow emission levels of lanthanide-doped materials and the close energies between the emissions involved. An alternative energy ratio that would solve this issue has been proposed, which uses thermalized states at the ground level, i.e. the ground state can thermally populate the first excited state. Thus, the same emission band is alternatively excited by two different excitation lasers, from the ground and the first excited states. This method is interesting because it facilitates data recording and analysis, but it requires two excitation sources and constant switching between them. Such materials have not yet been optimised for use within *in vivo* environments because they work exclusively in the visible range. In addition, thermalization of the first excited state is low at biological temperatures and thus, though suitable for measuring temperature changes within this range, one of the excitation wavelengths provides a low emission intensity that may be hard to distinguish in biological environments.[17]

Polarization anisotropy can also be considered as a ratiometric technique, because it compares emission intensities recorded under two different light polarizations. It shares the advantages of intensity ratios and is independent of the illumination power and the distribution of LNMs. However, this technique has been insufficiently developed in the biological context, probably because its temperature dependence is complex, being influenced by both fluid viscosity and luminescence lifetime. Still, the feasibility of the technique has been demonstrated, even in small animals, using the Green Fluorescent Protein (GFP) as the LNM.[18] Further work has been carried out, aiming to construct smaller probes based on proteins, which may soon push further development of this strategy.[19]

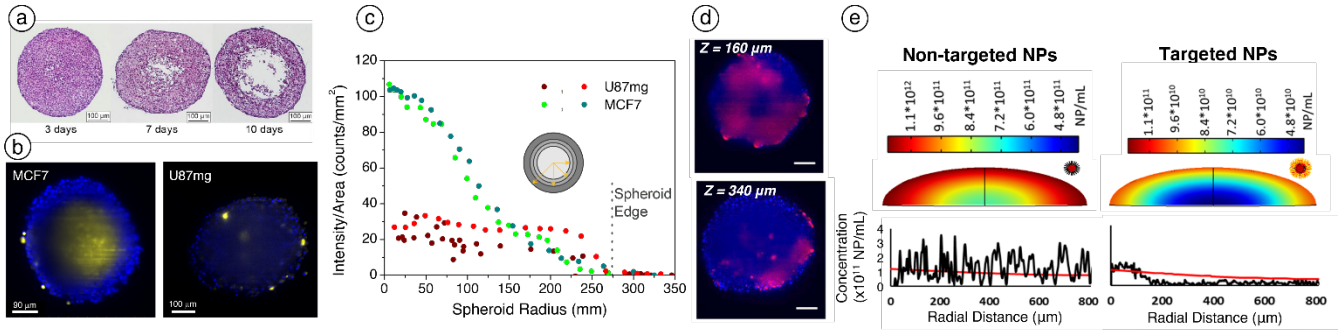

Figure 2. (a) Histology of human head and neck carcinoma cell line FaDu-formed spheroids, showing the characteristic necrotic core devoid of intact cells.[30] (b,c) Fluorescence microscopy images (b) and quantification (c) of propidium iodide penetration into spheroids made of breast (MCF7) and brain (U87.mg) cancer cell lines, showing the increased presence of propidium iodide (in yellow, labelling dead cells) in MCF7 spheroids of the same size and age as U87.mg.[32] (d) Cross section of a spheroid at 160 µm and 360 µm (equivalent to its maximum diameter), where blue colour shows DAPI fluorophore emission labelling cell nuclei and red shows emission from Nd^{3+}-based nanothermometers. LNM penetration is inhomogeneous over the spheroid surface. Scale bar: 100 µm.[32] (e) Experimental and computational models of the diffusion of polymeric fluorescent nanoparticles into a spheroid, using non-targeted and targeted NPs. Targeted NPs are sequestered at the spheroid periphery, whereas non-targeted NPs can penetrate (and leave) the spheroid easily.[31] Figures reproduced under the Creative Commons Attribution Licence (CC BY 4.0) from references 30, 31, and 32, with permission from MPDI, Nature Publishing Group, and Ivyspring International Publisher, respectively.

Finally, luminescence lifetime, i.e., the characteristic time an excited state requires to lose its population (see Equation 2), is also a robust parameter to be considered, as it is independent of both the concentration of LNMs and the illumination intensity. In addition, it requires measurement of a single emission wavelength, meaning that spectral distortions, often occurring when light is travelling through tissue, will not play a role. However, as a principal drawback, the experimental set-up is more complex, as it requires a pulsed laser and synchronized detection with time resolution.[20] Still, this technique has been extensively used and constitutes an interesting option, even in biomedical applications, first demonstrated with organic dyes[21] and more recently with inorganic nanoparticles such as Ag_2S.[22]

Nanothermometry in Practice

One of the first proposed applications of nanothermometry has been in the determination of intracellular temperature, to study cellular metabolism. Thermogenesis at the cellular level refers to chemical processes that cause local changes in temperature, as a response to endogenous stimuli. Typically, processes involving cellular metabolism are affected, and hence the mitochondria and surrounding cytoplasm are the most studied organelles.[10] Various sensing strategies have been explored to determine endogenous temperature changes occurring in live immortalized cells. Whereas most techniques address temperature changes of around ≤1 K for endogenous intracellular gradients and those due to external stimuli, more striking values close to 3 K (intracellular temperature gradient between the nucleus and cytoplasm), or 6 to 9 K (increase in temperature around mitochondria)[23] have also been reported. Such impressive gradients and changes in intracellular temperature understandably lead to speculation as to whether the probes, and the employed methods, are reliable. To put these results into perspective, extracellular temperature changes in cancer tissue are generally in the range of 1-2 K, as determined from consistent theoretical and experimental data. To better understand the putative range of temperature heterogeneity within a cell, Baffou *et al.* reported theoretical modelling of the expected thermal changes that occur during intracellular thermogenesis. By taking into consideration aspects such as heat diffusion by organelles, the size of mitochondria, their distribution throughout the cytoplasm, thermal conductivity of the plasma membrane, and the mass of glucose that can be transformed into heat, changes in temperature of the order of 10^{-5} K were calculated.[24] Similar theoretical values have been determined by other groups.[25]

This discrepancy between theoretical and experimental values (known as the 10^5 gap) makes us wonder about the limitations of each approach. Indeed, in a commentary discussion from 2015,[26] relating to the 10^5 gap, it was suggested that a limiting factor in experimental findings was the use, or rather lack, of accurate intracellular thermometers. Experimental limitations are largely based on the sensitivity of the measurement techniques and the adequacy of the implemented protocols, which can be affected by parameters other than temperature. Regarding theoretical modelling, sources of inaccuracy are insufficient data on the validity of the thermodynamic equations that apply in the complex cell environment, and the accuracy of the thermal constants used for cell components (thermal conductivity, mainly).[27] However, as more thermometric materials and sensing strategies have been applied to the measurement of intracellular temperature (fluorescent and non-fluorescent, a good summary can be found in reference 10), all providing consistent results, a higher reliability of experimental data is accepted. It should be noted that the maturity of *in vitro* thermometry has recently reached a point at which intracellular thermometric probes are commercially available, as well as detailed measurement protocols.[10] Applications of these probes include, for instance, understanding the mitochondrial thermogenesis in brown adipocytes,[28] which play an important metabolic role in non-shivering thermal regulation of many animals, including humans. From an applied perspective, their contribution to energy consumption makes them interesting targets in obesity treatment studies.

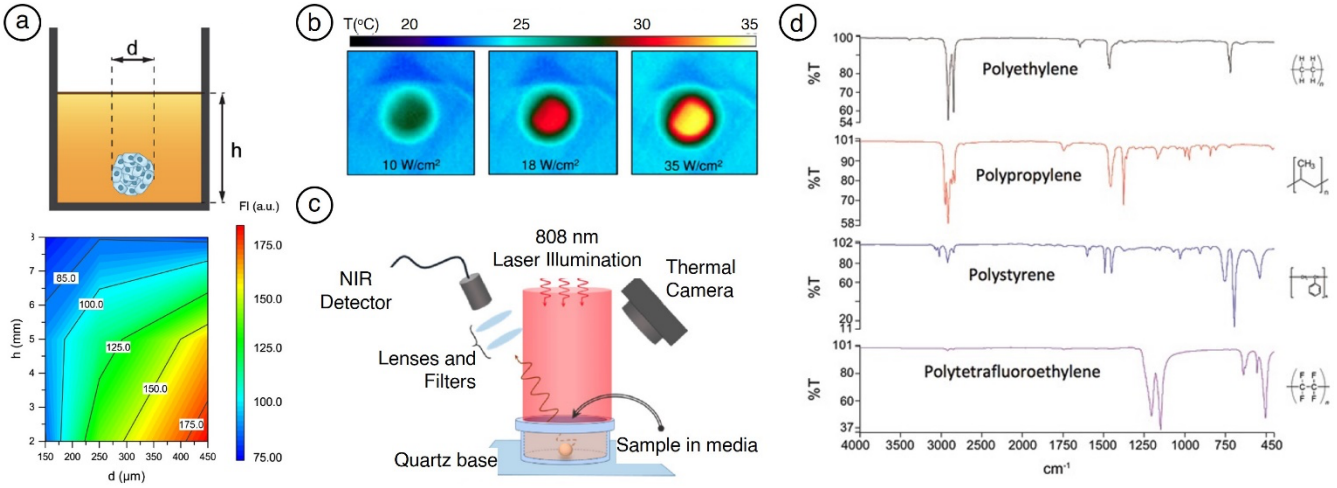

Figure 3. (a) Spheroid model of 150 to 450 μm in diameter, shown in a 96 well-plate (top), and the fluorescence intensity of ICG (NIR dye) as a function of the distance from the centre of the spheroid (bottom).[30] (b) IR thermal camera images of irradiated spheroids showing the poor spatial resolution of the technique. These images were taken using the experimental setup in (c), in which hyperthermia was achieved in spheroids treated with plasmonic nanoparticles and nanothermometers. Laser illumination at 808 nm is required for heating and luminescence excitation. Temperature was recorded using both, a thermal camera and nanothermometers emission.[32] (d) IR absorption spectra of the most common plastics used for the manufacture of the cell culture plates.[33] Figures reproduced under the Creative Commons Attribution Licence (CC BY 4.0) from references 30, and 32 with permission from MPDI and Ivyspring International Publisher, respectively.

Despite early controversy, *in vitro* nanothermometry has seen a fast evolution, reaching a stage at which it is being applied in biological research. However, thermal monitoring of more complex samples involves additional concerns, largely related to light-matter interactions, but also to the delivery of LNMs to the area of interest.

Nanothermometry in 3D cell models. It is generally accepted that 3D *in vitro* cellular models represent a suitable stepping-stone, or even a valid alternative to *in vivo* models, as long as physical aspects such as geometry and cellular heterogeneity are kept as close to the real tissue as possible. Indeed, advanced 3D cell models may even offer improved characteristics with respect to *in vivo* models, such as control over biophysical properties (including oxygen state and fluid flow) and the ability to genetically modify the expression of proteins at the single cell level.

As discussed above, a large body of information is available on mapping intracellular temperature changes using LNMs. However, few studies have attempted temperature measurements in 3D cell models such as spheroids, organoids, organ-on-a-chip, and 3D-printed tissues, all of which may provide extensive information as to how successful the use of LNMs may be *in vivo*. Two of the most critical aspects in the experimental design are the spheroid/organoid geometry, as well as the uptake and spatial distribution of the LNMs in or around the spheroid. Regarding organoid geometry, it is well known that the type and number of cells, or relative numbers of the various cell types when using heterologous cell mixtures, as well as the growth stage (number of days), are crucial factors that determine the overall size and shape.[29] Unfortunately, there is no rulebook that can be used to pre-define organoid size or shape, and therefore preliminary growth tests must be carried out. With increasing size and growth time, the interior core of the spheroid becomes gradually devoid of nutrients and there is a lack of gas exchange, which is crucial for the delivery and removal of oxygen and carbon dioxide, respectively. The resulting necrotic core, which can be distinguished using either fluorescence staining or histology (**Figure 2a-c**), features a different light absorption profile compared to the outer spheroid rim, due to the enhanced presence of cell debris and cellular heterogeneity.[30] In practice, few LNMs incubated together with spheroids will ever reach the internal core due to sub-optimal LNM physicochemical properties such as uncontrolled aggregation or sedimentation, both of which can be unfavourable for LNM-cell interactions. Also, the compact nature of the extracellular matrix and cell-to-cell interactions within the external layers of the spheroid may result in inhibited LNM penetration. Nanoparticle trapping within the external layers of spheroids has been described,[31] as has non-homogenous LNM distribution around the spheroidal periphery,[32] most likely due to LNM sedimentation during incubation. Examples of these aspects are shown in **Figure 2d,e.**

With regards to the experimental setup, the overall spheroid size and the spatial resolution of available IR cameras may determine the signal intensity recorded from LNMs. In work by Egloff-Juras et al.,[30] the use of a NIR camera (700 – 850 nm detection window) restricted imaging depths to a few mm and required spheroid sizes to be larger than 225 μm in diameter (**Figure 3a**). In contrast, a standard IR thermal camera can only provide information on the surface of spheroids immersed in a medium (i.e. on the liquid), and thus cannot distinguish temperature changes through the spheroid (**Figure 3b,c**). As opposed to IR cameras, the detection of light emitted by LNMs for thermometry involves the arrangement of laser excitation sources and detectors in a similar location above the sample to be interrogated, which may complicate the setup (see **Figure 3c**). Thus, any barriers

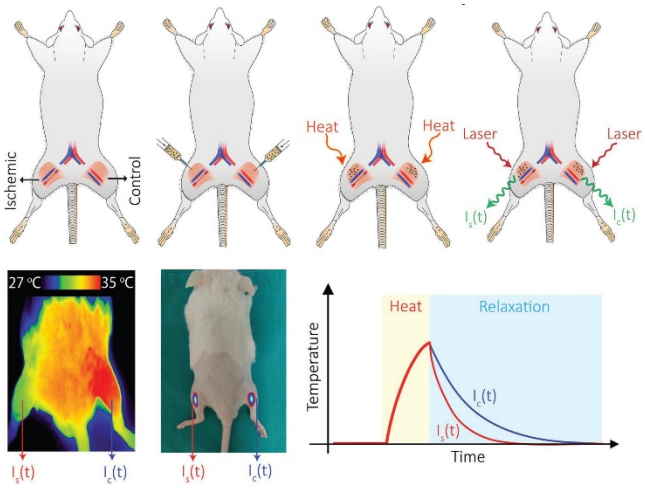

Figure 4. Mouse model in which ischemia was generated in the left leg. Due to the ischemic episode, the temperature of the limb was lower, which was detected using a NIR-based nanothermometer through the transient thermometry (TTh) method. Reproduced from reference 37, with permission from John Wiley and Sons Publishing.

that may hinder light transmission (including the cell medium) should be considered. In particular, the presence of polystyrene (PS) and polypropylene (PP) plastics typically used in cell culture, for example in microplate lids, causes a significant reduction of light transmission through the IR camera detection window (**Figure 3d**).[33] Whilst this may be problematic for NIR cameras and hence detection of heat release, it also poses a problem for incident NIR light sources typically used for LNM measurements. For example, a 10% reduction in power density can occur upon irradiation with a NIR laser source (808 nm), which is significant for experiments in the biological range (*ca.* 30 – 50 °C), where a temperature increase of a few degrees can result in cell death. This issue reiterates the importance of conducting appropriate controls and taking into account all components that may cause light scattering or absorption.

***In vivo* and *ex vivo* tissue.** Attempts to apply nanothermometers to real tissues appeared early in the development of the field, aiming to demonstrate that detection of the signal is possible. To simplify tissue-related complications, most studies started by using phantom tissue (a preparation with optical absorption and scattering resembling that in real tissue) or *ex vivo* animal models (most often chicken breast, but not exclusively). Phantom tissues have been developed to mimic tissue properties at specific wavelengths, also within the BW (mainly BW-I). The current catalogue of recipes covers a large number of options, including phantom breast, bone, cartilage, skin, arterial tissue, etc., so versatility is high.[34] The use of phantoms guarantees a high reproducibility in the experiments, due to their homogeneity and control over the shape and thickness of the sample, which is not always possible with *ex vivo* tissue. However, they do not resemble the chemical environment of real tissues, which would require using *ex vivo* tissues. Chicken breast is a homogenous tissue with reduced absorption properties and provides a sufficient thickness to study laser penetration depth. It should be noted that, commercial chicken breast shows a large variability regarding retention of liquids, meaning that the optical properties may vary between samples, but also that injected LNMs may spread differently depending on the degree of hydration. Obviously, this variability may cause inaccuracies in model design and temperature readout, as LNM concentration in a certain area may change. For the same reason, the way nanothermometers are administered is also important; injection into chicken breast (essentially an intramuscular injection) without backflow is crucial to effectively deliver the LNMs (or any other NP, for that matter). Partly due to the high current incidence of diabetic population who require daily injections, the methods and properties of intramuscular injections have been extensively studied. Whereas it is recommended to insert needles at a 90º angle to the tissue surface, the length of the needle (and hence the depth of injection) is largely dependent on the aim and precise location of the injection. The "pull-back" technique, developed to ensure that needles do not pierce blood vessels, involves insertion of the needle followed by aspiration, prior to expulsion of the syringe contents. Naturally, in *ex vivo* tissues such as commercial chicken breast, no blood would be expected, but the process of inserting a needle to create a channel, prior to expulsion of the contents, can still be useful. Other methods such as incision or biopsy punches are interesting alternatives, as they produce cavities of controlled dimensions.

These principles also apply to experiments using *in vivo* models. It should however be noted that the administration route in this case primarily depends on the disease model of choice. For the purposes of tumour hyperthermia, *in vivo* models should ideally involve the administration of LNMs intravenously or directly into the organ of interest. In contrast, in studies in which minimum tissue interference and controlled NP concentrations are required, subcutaneous or even intradermal injections may be most appropriate. An important consideration in all cases is the maximum permitted volume, which can vary as much as 10-fold, depending on the administration route and animal model.[35]

To some extent, the theory applied to nanothermometry *in vitro* can also be translated to *ex vivo* or *in vivo* applications. Notwithstanding, the complexity of tissues and organs in terms of geometry and interaction with light, restricts the use of nanothermometry to proof-of-concept experiments, rather than diagnosis. Yet, some promising results have been reported. One example is the exploration of LNM-quantum dots (QDs) composed of cadmium telluride (CdTe), to detect temperature changes at the nanoscale in *ex vivo Drosophila melanogaster* skeletal muscle samples. In this case, the nanosized LNM-QDs (2 nm) could bind to myosin and detect heat released during myosin-mediated ATP hydrolysis, via emission intensity measurements in the visible range (*ca.* 520 nm).[36] QDs have also been explored to study tissue relaxation dynamics in an ischemia murine model. Ximendes *et al.*[37] developed a technique to detect either temporal or permanent restrictions of blood supply that can lead to a shortage of oxygen in certain areas of the body, as it occurs in ischemia. As such, the biophysical properties of the relevant tissue are affected, including their thermal relaxation dynamics, which can thus be measured

using TTh (**Figure 4**). In this technique, the tissue is first heated up to subsequently measure how temperature decreases back to the equilibrium state. In the clinic, however, transient temperatures are typically monitored using IR thermal cameras, which are only reliable for superficial tissues, thereby preventing the extensive application of TTh.

Hence, the authors designed a nanothermometry detection system in which temperature-sensitive LNM-QDs (PbS/CdS/ZnS) were injected into the site of interest. As the emission intensity of these QDs depends on temperature, irradiation at 800 nm (an efficient excitation wavelength) and detection over time of LNM-QD emission at *ca.* 1200 nm, allowed the localization of damaged tissue. A similar TTh strategy has been applied to the early detection of cancer in mice, in this case using intratumor injection of Ag_2S NPs with high thermal sensitivity.[38] These particles were excited at 808 nm, with emission at 1200 nm, i.e., within the first and second biological windows, respectively. Heating required to induce the TTh effect was provided by simultaneous laser irradiation at 810 nm, using a higher power than that for photoluminescence excitation. The characteristic changes in tumour microvascular thermal relaxation properties could be used to differentiate it from healthy tissue. The findings showed an impressive diagnostic ability, as tumours could be identified up to 7 days prior to optical detection.

A final illustrative example of nanothermometry *in vivo* is provided by the measurement of brain temperature in mice, upon injection of Ag_2S NPs. Again, by using excitation and emission wavelengths of 808 nm and 1200 nm, respectively, measurements could be recorded in a non-invasive manner through the skull and scalp. Although thermal calibration was performed with the particles inside an excised brain, so as to mimic the experimental environment, conclusions still relied on thermal variations, as expected for a sensor based on luminescence intensity. A thermal resolution of ± 0.2 °C was estimated. As shown in **Figure 5**, this proof-of-concept experiment was designed in a way that it nicely underlined the differences between measuring temperature *in situ* (brain temperature) or externally through an IR thermal camera (skin temperature). The results suggested that externally induced temperature changes (whole body cooling) caused activation of thermal regulation at the organ level (in the brain), to reduce the impact of temperature in a homeostatic method. Thus, thermal changes were up to three-fold larger on the skin (10 K) than in the brain (3 K). In contrast, when thermal changes were triggered directly inside the brain through a barbiturate coma, thermal change was exclusively observed in the brain, without any external impact on the skin, so it could only be detected through the nanoparticles.[39]

In the above examples, temperature was deduced from the evolution of the emission intensity from luminescent nanoparticles. These techniques are valid to determine how temperature changes over time, but cannot provide absolute temperature values, which would require knowing exactly to what extent light gets absorbed by tissue along the way. Besides, this method assumes that the concentration of nanoparticles in the spot of interest remains constant during

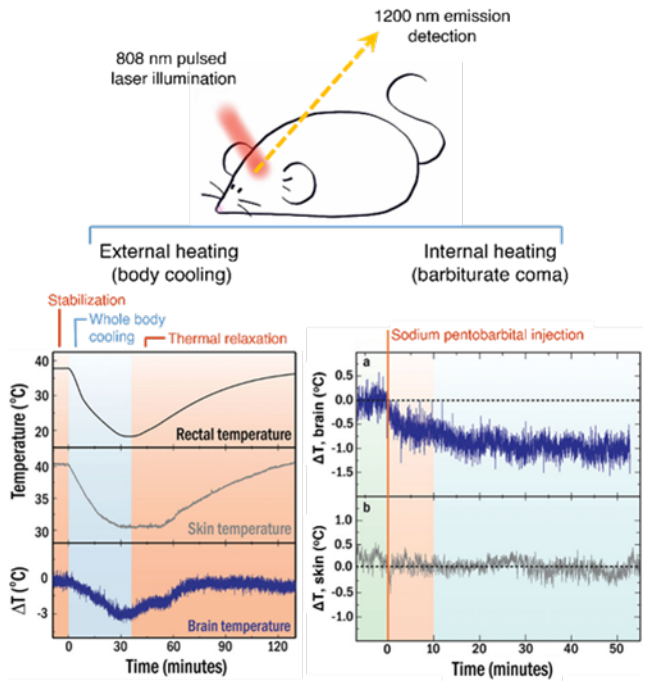

Figure 5. Brain thermometry through skull and scalp measured with Ag_2S nanoparticles emitting in the BW-II (at 1200 nm). Brain temperature is compared with skin temperature measured with a thermal camera, and rectal temperature measured with a thermocouple. Reproduced from reference 39, with permission from John Wiley and Sons Publishing.

the measurement, and requires that the tissue through which light penetrates does not change over time due to the measurement itself. Additionally, the TTh technique also requires control measurements involving healthy tissue. When all of these aspects are taken into consideration, it is clear that nanothermometry measurements *in vivo* are far from simple, and although LNMs can provide advantages such as local delivery and improved sensitivity, ultimately a critical eye must be taken in deciphering the true values.

Beyond diagnosis: hyperthermia. Techniques such as radiofrequency or microwave ablation are commonly used to induce tissue necrosis of solid tumors, especially in liver cancers. In both methods, localized heat is induced via insertion of a probe into the diseased tissue, so that sufficiently high local temperatures are achieved. During treatment, a fine control over the applied temperature is crucial to avoid excessive damage to surrounding healthy tissue, and therefore thermocouples or optical fibres are used to determine temperature changes *in situ*. However, these sensors suffer from limited spatial resolution and are intrinsically invasive, two limitations that can in principle be solved with nanothermometry.

Interestingly, various types of nanoparticles can transform incident electromagnetic radiation into heat released to their local environment. This effect is mainly achieved by using plasmonic nanoparticles illuminated at their localized surface plasmon resonance (LSPR) and magnetic nanoparticles subjected to alternating magnetic fields. In the case of plasmonic nanoparticles, heat release is due to the large absorption cross-section at the plasmonic resonance wavelength. At this wavelength, surface electrons

participate in a synchronized oscillation, known as a plasmon, whose energy can be eventually released to the environment in the form of heat. Regarding magnetic nanoparticles, alternating magnetic fields are transformed into heat in different ways, including energy losses during magnetization-demagnetization cycles (associated to hysteresis loops), and losses linked to a flipping movement of the particle (Brown relaxation) or its magnetic moments (Néel relaxation).

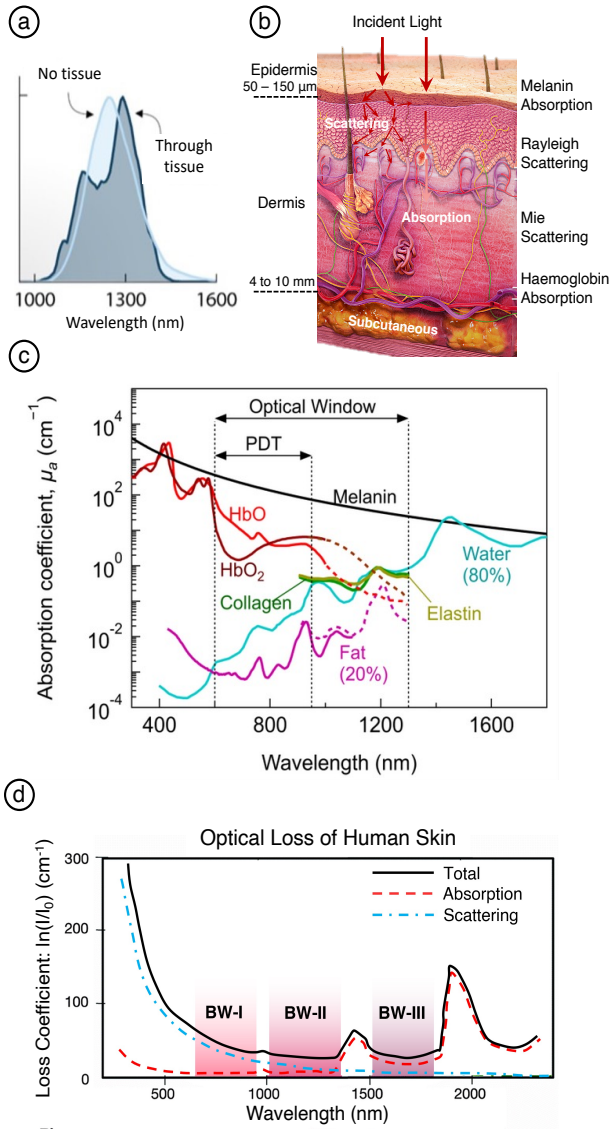

Figure 6. (a) Distorted NIR emission from Ag_2S nanoparticles measured through tissue, compared with the emission free from tissue interference.[46] (b) Schematic view of the skin, showing the main interactions with electromagnetic radiation at different depths, and pointing out the most important causes of optical losses.[47] (c) Main biological molecules and their absorbances in the Vis-NIR electromagnetic range.[48] (d) Optical losses in the NIR for a standard model tissue, showing the biological windows (BW) and differentiating absorption and scattering losses.[53] Figures reproduced under the Creative Commons Attribution License (CC BY 4.0) from references 46, 47, 48, and 53, with permission from John Wiley and Sons Publishing, Wikipedia, MDPI, and The Royal Society of Chemistry, respectively.

Such nanoparticles, which we term nanoheaters, are interesting choices for the induction of coagulative necrosis in tissues, as well as for other heating applications (see section on cryopreservation below), because they would minimize the invasiveness of localized hyperthermia. In principle, it is also possible to generate heat from some LNMs, which would thereby act as both nanothermometers and nanoheaters, simultaneously. However, this process would involve simultaneous radiative and non-radiative energy processes, the latter requiring significantly higher power densities to achieve sufficient heating. Alternatively, co-administration of nanothermometers together with nanoheaters offers an exceptional flexibility in the design of the system (including excitation range, NP size, surface charge, colloidal stability, etc.). Although simply mixing nanoheaters and nanothermometers could indeed be sufficient to detect local heating upon externally applied electromagnetic excitation, biological systems are affected by aspects such as protein corona formation, EPR effect, or size-dependent cellular uptake. As a result, co-administration is unlikely to result in co-localization of nanoheaters and nanothermometers. Consequently, a more interesting alternative that offers considerable flexibility in the design of the nanoparticle system, is the mutual binding of nanoheaters to nanothermometers via either covalent bonds or electrostatic forces, or even using encapsulation techniques. Approaches toward covalent binding must take into consideration the length of linker molecules or the growth of an intermediate shell, because photoluminescence quenching by nanoheaters may occur. A potentially simpler approach comprises the encapsulation of both nanoparticle types within a biologically compatible shell, such as a polymeric coating. Indeed, the dual encapsulation approach further protects LNMs from any undesired protein corona formation. The protein corona, increasingly termed biocorona because it includes other molecules such as lipids and nucleic acids, has likely a more important effect in altering the amount of LNMs that are delivered to the site of interest, as opposed to directly altering the luminescence readout. Still, it may have some influence, as will be discussed in the section devoted to the particle microenvironment.

Beyond diagnosis: Cryopreservation. The work by the Bischof group aimed at bringing the heating properties of highly absorbing NPs to the forefront of biomedicine, by applying them in the rewarming of cryopreserved tissue.[40-42] Specifically, the technique involves the perfusion of tissues and organs, prior to cryopreservation, with a colloidal dispersion of gold NPs featuring a LSPR in a BW. In the presence of chemical cryoprotectors, the tissue sample is vitrified following a critical cooling rate (CCR), specific to the amount and type of cryoprotector. To rewarm or devitrify the sample, rapid warming must take place to avoid any cell damage due to the formation of ice crystals during the devitrification stage. Such a rapid rewarming can be achieved via resonant excitation of a plasmonic mode in gold NPs, reporting rewarming rates above 10^7 K/min, which are considered to be the gold-standard to avoid crystallization.[40] However, it should be noted that the experimental setup relies on a thermocouple that is inserted into a droplet of less than 1 µL, allowing biological sample diameters up to 1 mm in diameter only. Whereas the thermocouple offers an

inexpensive and fast method to detect temperature changes, its level of accuracy is low (≈ ± 2.5 K RMS).[43] Indeed, such a degree of accuracy is irrelevant in the context of rewarming cryopreserved samples where temperature changes are nearly 100-fold higher. However, in the case of photoablation where a few degrees can determine whether cellular necrosis occurs or not, or for temperature-based measurements of cell malignancy, inaccuracies of ± 2.5 K are disproportionate. Again, the use of LNMs as a suitable alternative has gained increasing interest due to its accuracy and biocompatibility. Specifically focusing on *in vitro* biological models being exposed to external electromagnetic radiation, the amount of available data is surprisingly small. Conceptually, the simultaneous application of nanoheaters and nanothermometers is not complicated, yet most studies in which photoablation is monitored *in vitro* rely on temperature measurements using an infrared camera. Hence, we should ask the question of why nanothermometers are not used more often. The answer may come from the difficulties in delivering sufficient LNMs to the site of interest, so that the LNM signal is strong enough. A second possibility relates to the structural and biological complexity of the tissue itself, which has an important effect on the intensity of both incident and reflected light, hence questioning the reproducibility of LNMs (disused in further detail below).

Performing the Experiment: How Accurate Is the Measured Temperature?

Most studies related to 2D intracellular *in vitro* temperature measurements are performed using NP probes, some of which are commercially available.[10] With the exception of transfection agents, most temperature nanoprobes enter cells via endocytosis. Once located intracellularly, temperature measurements can be made using a fluorescence microscope, a plate reader, or a spectrofluorometer, for fluorescence emission readout. Such readings must be compared with a previously obtained calibration curve. Thus, the light detection system and the medium used for both the calibration curve and the *in vitro* measurements must be identical, which often involve highly complex media containing high quantities of glucose, amino acids such as glutamine, and albumins or other proteins. Whilst mammalian cells can be studied in transparent buffers with adjusted ionic strength and pH, these are significantly different to their usual environment and therefore might result in undesired stress, which would manifest itself as a temperature change. Therefore, any LNM must ideally be stable in complex media and compatible with visible-light detection techniques, which would drastically facilitate their use in standard commercial set-ups available in most biology laboratories.

On the other hand, application to *in vivo* studies requires that the stability, size, and surface chemistry of nanothermometers be carefully controlled, to avoid unwanted non-specific removal from the circulation via the reticuloendothelial system (RES), and to accumulate at the site of interest. Such an accumulation may require the use of targeting molecules such as antibodies or aptamers, or simply be based on the so-called enhanced permeability and retention effect (EPR), which is known to occur in tumours.[44] From the spectroscopy perspective, conditions are also demanding, as the LNMs must be as bright as possible and their excitation and emission wavelengths match one of the biological windows, for best penetration combined with minimal harm. Furthermore, when heating is aimed at producing hyperthermia, a common problem is the dissipation of heat due to blood flow. Obviously, this is highly dependent on the tissue of interest, highly oxygenated organs being more affected. The opposite may also happen, as poorly oxygenated tissues, such as dense tumours, cause a heat-sink and inhibit heat dissipation. Therefore, accurate temperature measurements become even more relevant. However, can we trust the thermal readout obtained from nanothermometers? Although thermal monitoring has been demonstrated in small animals, it is still a matter of debate how nanothermometers, or more specifically, their emitted light, should be recorded and processed to provide accurate thermal information. Indeed, several factors limiting the accuracy of the measurements have been identified, which may hinder the adequacy of the calibration curve, thereby compromising the thermal readout.

Limitations associated to the light path: the tissue issue. One of the most important aspects of *in vivo* experiments is related to tissue scattering and absorption,[45] as on one hand, these reduce the fluence of incident light reaching the nanothermometer and, eventually, the nanoheater; and on the other hand they can change the spectral shape of luminescence (**Figure 6a**).[46] The same can be said for the luminescent signal emitted by the nanothermometers in question, which must be recorded with a sufficient signal-to-noise ratio, to guarantee a meaningful thermal readout. In general, absorbance is caused by soluble components present in the intra- and extra-cellular environments, whereas scattering occurs due to the physical organization of the tissue, which leads to refractive index contrast (**Figure 6b**).[47] Both effects are remarkably dependent on wavelength. In the case of absorption, the spectral range is defined by the allowed electronic transitions in molecules, and thus strongly depends on chemical composition. The absorption spectrum of a tissue will thus depend on the concentration of each component, haemoglobin and water typically making the main contributions (**Figure 6c**). However, for some tissues, melanin and yellow pigments (β-carotenes and bilirubin) play a major role in the visible range, while fat and adipose tissue contribute in the NIR.[48,49]

Absorption is important, not only because of the optical losses in the light beam, but also because the absorbed optical energy is then transformed into a different type of energy, most often into heat, thereby leading to an increase in local temperature. A maximum illumination dosage (power and time) to avoid tissue overheating has thus been defined (guidelines are regularly published and updated by the International Commission on Non-Ionizing Radiation Protection, ICNIRP)[50]. Alternatively, absorbed energy can be released radiatively, in which case the tissue itself presents light emission, constituting what is known as autofluorescence. Just as light emission does, autofluorescence may overlap in the detector with the emission from LNMs and cause problems, including

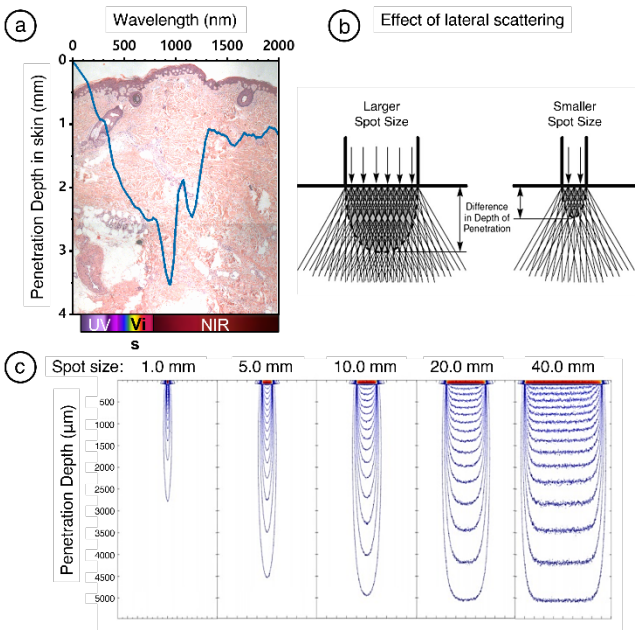

Figure 7. (a) Light penetration depth in human skin, overlaid on a histological cut stained with eosin and haematoxylin, showing the biological structures that light can reach depending on its wavelength. (b, c) Dependence of the penetration depth of light, ranging from 525 to 1100 nm, as a function of the incident beam diameter. Reproduced under the Creative Commons Attribution Licence (CC BY 4.0) from reference 56, with permission from Springer Nature.

uncontrolled background signal or additional emission bands that may hinder those used for thermometry. Fortunately, most endogenous components of *in vivo* and *in vitro* biological samples display autofluorescence in the blue-green optical range and thus it does not represent a significant issue for measurements within the biological windows. However, autofluorescence in the NIR has also been reported, e.g. associated to melanin or chlorophylls, which are present in commercial food for experimentation animals,[50] oftentimes even if labelled as "fluorescence free". It is thus important to be aware of the expected composition of the tissue under study and its potential autofluorescence, to avoid misinterpretation of thermal data.[51]

For scattering, on the other hand, the degree of interaction depends on the relative size of tissue fibrils, cells, or other obstacles for light, compared to the wavelength of incident light. Traditionally, two scattering modes are described: Rayleigh scattering, when the obstacle is significantly smaller than light wavelength; and Mie scattering, when both dimensions are in the same range. For longer wavelengths, scattering becomes negligible, which for tissues applies in the NIR (**Figure 6d**).[53] In summary, both Rayleigh and Mie scattering contributions should be considered to optically describe a tissue, even though often one of them dominates over the other. For instance, fatty tissues or brain tissue are usually dominated by Mie contributions, whereas the skin and other fibrous tissues display predominantly Rayleigh scattering.[52]

The exact light attenuation (a term that includes both scattering and absorption) will thus vary for different tissues. However, a generic spectrum can be approximated as shown in **Figure 6d**, where the biological windows can be clearly identified. It is well documented that successful penetration of light through *in vivo* environments, with multiple tissue boundaries, requires the selection of wavelengths within one of the BWs, in the NIR. By focusing light within these BWs, the absorbing properties of water, haemoglobin, lipids, etc. are partially avoided,[54] thereby allowing the maximum energy to be transferred to the site of interest. The characteristic length that light of a certain wavelength can travel through tissue is known as penetration depth. Since light intensity can be assumed to decay exponentially in the propagation direction, the penetration depth is typically defined as the characteristic distance of the exponential decrease (i.e., the distance at which the normalized intensity decays to 1/e times its initial value). Penetration depth varies with wavelength,[55] for the reasons discussed above, and is obviously longer for light within the biological windows (**Figure 7a**). However, it also depends on illumination conditions such as spot size, because lateral scattering of the light beam is less relevant for bigger spot sizes (**Figure 7b**). As an example, Monte Carlo simulations applied to light-tissue interactions through skin show that maximum penetration is reached for a 10 mm beam width, while a further increase of the beam size does not have any additional effect on penetration (**Figure 7c**).[56] Considering all of the above discussion, at the time of designing an experiment it is important to select an appropriate wavelength within the biological windows, but also to consider the maximum illumination dose that can be used to avoid tissue damage, and even to select the appropriate size of the illuminated area and improve penetration depth.

The extent of scattering and absorption varies in tissues, between healthy and diseased states. Of significant concern are changes in scattering and absorption that may occur *in situ*, due to an applied therapeutic treatment.[57] In thermal ablation techniques, it is well-known that real-time monitoring is required to control excessive heating, which may easily cause undue damage to surrounding tissues. A wide range of cellular and molecular changes can take place, including protein denaturation, cell membrane damage, production of apoptotic bodies, changes in osmolarity, etc., all of which can in turn enhance scattering and absorption of both excitation and emission light.[58] This may also happen, for instance, during the measurement of transient temperatures in TTh, as a preliminary heating step is required prior to recording the cooling curve that provides tissue information. To study the extent of such a change, Lifante et al. used Ag_2S semiconductor nanoparticles (13 nm diameter), specifically prepared to display a lower photoluminescence quantum yield, but a high heating efficiency instead. Upon injection in mice and illumination at different powers, a range of target temperatures to measure TTh curves was obtained. From the results, it was concluded that the characteristic relaxation time varied with temperature, which could be correlated to a different heat diffusion within the tissue. Based on numerical modelling, it was concluded that changes were produced in the tissue at the higher illumination powers, which could be ascribed to changes in blood perfusion through tissue.[59]

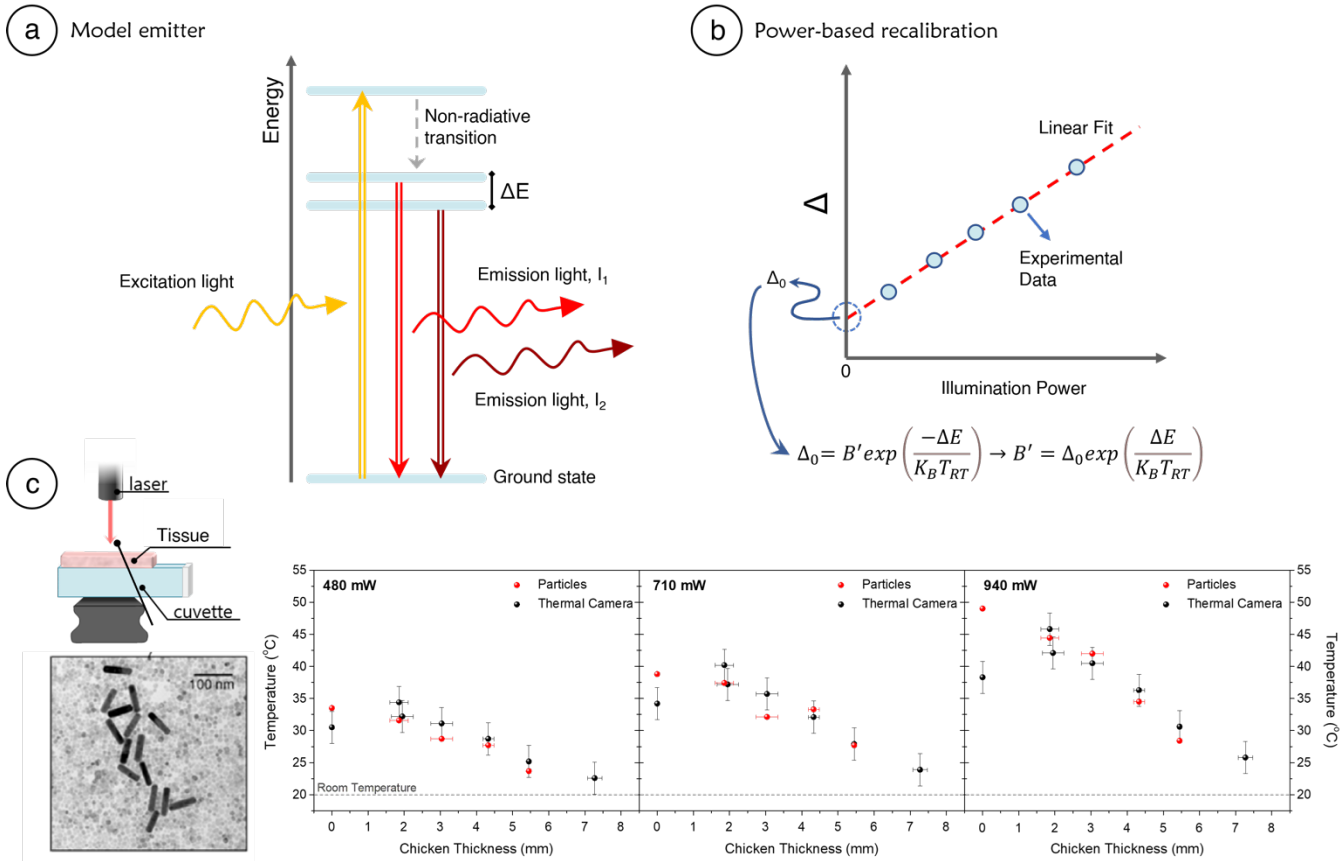

Figure 8. (a) Example of a diagram of energy states with thermalized levels. (b) Scheme for the recalibration of B, based on the dependence of the intensity ratio with illumination power. (c) Model *ex vivo* experiment, comparing temperature measured through tissue and externally with a thermal camera. Reproduced with permission from reference 60, American Chemical Society.

The need to recalibrate. The absorption and scattering of light by tissue, even within the biological windows, represent a major source of inaccuracy in optical nanothermometry. This is most clear in the case of intensity-based thermometers not calibrated *in situ*, which can only be used to obtain transient temperatures, as long as neither the tissue properties nor the NP distribution changes during the experiment. If we shift from one-intensity to intensity-ratio thermometry, inaccurate control over excitation light or NP distribution would no longer be an issue. However, both scattering, and absorption depend on wavelength, thus the shape of the emission spectrum may change along the path of light through tissue (**Figure 6a**). The spectral distortion becomes more significant in thicker tissue, but it will also depend on other tissue features (blood flow, percentage of fat, melanin, etc.). Consequently, working at two different wavelengths generates the drawback that each of them will interact differently with the tissue. As a result, if the calibration of the intensity ratio has not been performed in situ, it will most likely not be valid in the final experiment. Unfortunately, calibration requires measuring the emission spectrum along the whole thermal range of interest (commonly from room temperature up to 50 or 60 ºC, at least), which is not viable during diagnosis or therapy. Besides, conducting multiple calibrations is a time-consuming task, which is not the most convenient situation in biomedical experiments.

Solutions to the above issue have been proposed by using intensity ratios in thermally linked states of lanthanide-doped nanoparticles. The procedure involves a preliminary calibration in a controlled environment, which will be subsequently adapted to the final experiment *in situ*, following simple steps that do not require heating the sample to specific set points. This is possible because, in thermally linked ratios, two states share the electronic population, with a distribution that is described by a Boltzmann function. Therefore, their emission intensities are also linked through the same law, and the intensity ratio can be described as:

$$\Delta = \frac{I_1}{I_2} = B \cdot e^{\left(\frac{-\Delta E}{k_B \cdot T}\right)} \quad (3)$$

Here, Δ is the thermal parameter to be calibrated, i.e. the ratio between intensities I_1 and I_2 (**Figure 1c**), I_1 being the intensity of the most energetic state and I_2 the intensity of the least energetic one (**Figure 8**); K_B is Boltzmann's constant, T the temperature and ΔE is the energy separation between the barycentres of the two involved energy levels (**Figure 8a**).[60] Finally, B is a value that depends on spectroscopy parameters such as the degeneracies of the involved states, their spontaneous emission rates, and their average spectral frequency. In the first reports using this formula,[61] the definition of B also included the wavelength dependence of the detection system response, which is fair because it also affects the recorded spectrum. However, this consideration was made assuming a homogeneous, transparent medium between the emitting sample and the detector. If, instead, light travels through a non-transparent

medium, the spectrum will be distorted as discussed above, in turn leading to a change in the B value. Thus, B is the parameter that must be recalibrated in situ, whereas ΔE can, in principle, be considered constant (note that, in lanthanide-doped crystals, this consideration is accurate because of the shielding of the 4*f* orbital).

This technique was first applied by Balabhadra et al., who showed the relevance of this effect on the calibration curve of $SrF_2:Er^{3+},Yb^{3+}$ nanothermometers in different solvents.[62] The proposed method comprised a first thermal calibration of the emission, to determine ΔE. Upon transfer of the particles into a different solvent, B was re-evaluated through a study of emission as a function of power, which is simpler because it does not require accurate thermal control. As any solvent will typically absorb some light, it will heat up mildly, in a way that Δ follows a linear dependence with the intensity ratio.[63] Thus, a linear fit of Δ versus illumination power allows determining Δ_0, i.e. the intensity ratio at room temperature, T_{RT} (**Figure 8b**). This value of Δ_0 can then be used to define the required new B, which we denote as B' (**Figure 8b**) as:

$$B' = \Delta_0 \cdot e^{\left(\frac{-\Delta E}{k_B \cdot T_{RT}}\right)} \quad (4)$$

With this new B' parameter it is now possible to accurately measure temperature in the new solvent, with no need to change the temperature externally. This technique has also been tested for both excitation and emission light beams travelling through *ex vivo* tissue (chicken breast, see **Figure 8c**).[62] In this experiment, an aqueous colloidal dispersion, containing a mixture of $CaF_2:Nd^{3+},Y^{3+}$ nanothermometers and gold nanorods, was prepared to simulate a hyperthermia experiment. The mixed dispersion was poured into an optical-glass cuvette, which could be readily monitored with a thermal camera. Both Nd^{3+} ions and gold nanorods could then be excited with a laser at 808 nm, within the BW-I. The Nd^{3+} emission at 1050 nm (BW-II) was recorded during irradiation, to measure temperature changes. The results showed a good agreement between thermal readouts from the nanoparticles and from the IR camera. However, both values only matched if B was readjusted following the protocol explained above. Otherwise, differences as large as tens of degrees would have been detected when light was travelling through only 5 to 6 mm of tissue.

Aiming for a one-step process when nanothermometers are administered into a biological sample, the same group tested an alternative option for readjustment of B. The experiments were performed *in vitro*, using 3D tumour spheroids immersed in cell media, which had been previously treated with a hybrid probe comprising polystyrene colloidal spheres covered by both $CaF_2:Nd^{3+},Y^{3+}$ nanoparticles (nanothermometers) and gold nanostars (nanoheaters).[32] The measurement protocol in this case was based on monitoring the evolution of temperature upon turning the illumination on, which was found to follow an initial fast increase before slowly reaching a plateau. The first ramp could be fitted to a straight line, which at time zero would provide the value of Δ_0 needed to calculate B'. The main advantage of this method is that it avoids the need for a preliminary power calibration, which is an asset in hyperthermia experiments.

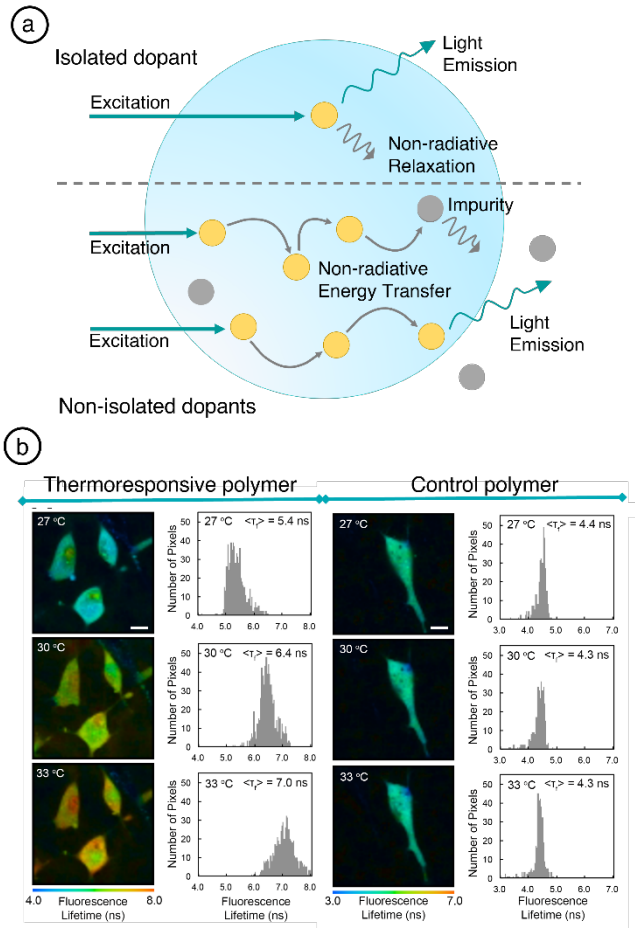

Figure 9. (a) Different mechanisms affecting photoluminescence intensity and lifetime, as described in the text. Note that all available processes compete. (b) Thermal maps calculated from LNM fluorescence lifetime. Reproduced with permission from reference 21.

However, it does require that the system can record several data points during the first minute of illumination, which is not always possible if the luminescence signal is too weak.

In fact, although these techniques solve the problem caused by the interaction of emitted light with tissue, the fact that they are based on lanthanide-doped nanoparticles, whose luminescence is often weaker than luminescence derived from other types of LNMs, precision and penetration depth are hindered. For instance, **Figure 8c** does not show thermal data from LNMs emitting from under a tissue thicker than 5.5 mm, as the measured signal in such experiments showed low signal-to-noise ratios. Besides, equation (3), which allows the described recalibration protocol, also involves a limitation regarding the sensitivity of the technique, which is defined by ΔE and B.[20] Thus, whereas many materials might not have enough sensitivity for intracellular temperature readings, it is generally enough for therapeutic and diagnostic applications.

We have seen in this section that thermometry methods based on either intensity or parameters that vary with wavelength (bandwidth and peak position) should be applied with care, taking into consideration the varying response of biological tissue at different wavelengths. This is especially important for calibrations being performed out of the final

experimental situation, which may not sufficiently represent the real environment. Additionally, if harsh conditions are applied to the tissue, either due to a disease condition or because of a therapy, optical and heat diffusion properties of the tissue may change, even during the treatment itself. It should be noted that emission lifetime is in principle the one property that is independent of tissue attenuation, because lifetimes are measured at a specific wavelength and thus not affected by spectral variations. However, the spectral distortion of light travelling through tissue is not the only reason why calibrations may lose significance. Indeed, the actual microenvironment where the LNMs are to perform may also influence their optical properties, lifetime in particular.

Limitations associated to the microenvironment. When we introduced above the main emission parameters in luminescence thermometry, we explained that an excited state can release its energy both radiatively and non-radiatively, and that the probability of each process is given by the rates k_r and k_{nr}, respectively. Both k_r and k_{nr} define the photoluminescence quantum yield of the fluorophore, η, and its experimental lifetime, τ_{exp}, as given by equations (1) and (2). As mentioned above, in the simplest scenario of an isolated luminescent atom in a perfect crystal matrix, the direct link between k_{nr} and temperature triggers a thermal dependence of η and τ_{exp}. However, further than temperature, are these parameters related to other environmental features?

In most materials, the situation is not as simple as the one described above. Continuing with the example of the dopant in a crystal matrix, if we increase the concentration of dopants to the extent that we can no longer consider them as isolated, new relaxation paths arise (**Figure 9a**).[64] In this case, energy can travel from one dopant to another through non-radiative energy transfer processes. Alternatively, some crystal impurities with additional vibrational modes can enhance k_{nr} if they are present in the surroundings of the dopant. Both non-radiative energy transfer and additional vibrational modes will reduce then the emission quantum yield and are thus called quenching routes. These additional relaxation routes are more likely to occur as the distance between the quencher and the luminescent dopant is reduced. Although the threshold proximity is different for each interaction, as a reference we can say that it is typically in the order of few nm. A final effect to be considered is the potential modification of transition rates due to alterations of the local electromagnetic field, including e.g., defects in the crystal matrix, such as strain, which trigger variations of the crystal field. However, the presence of external fields should also be considered, especially when plasmonic nanoparticles are used to enhance the emission intensity of nearby fluorophores.

Keeping this general overview in mind, it is straightforward to see why the environment around LNMs can strongly affect their luminescence properties. Sticking to the dopant example, the small size of NPs imposes interactions of the luminescent dopant, not only with other atoms in the particle itself, but also with atoms or molecules in the surrounding medium (**Figure 9a**). In terms of optical sensing, this means that the properties of the sensor, including the thermal calibration for temperature determination, may change if the environment does. In applications where the environment is homogeneous this is a negligible problem, as the effect will be the same during the experiment and the calibration. However, heterogeneous and complex environments, such as those found *in vitro* and *in vivo*, represent a major challenge because modifications to k_r and k_{nr} are hard to predict. This includes the fact that, upon introduction in the biological environment, a biocorona directly surrounding the particle will be formed, with a composition that will depend on the availability of molecules at the specific location of the particles, but also on the NP surface charge. Considering that the use of LNMs in biological environments is relatively recent, little data are available on the direct effect of the biocorona on optical sensors or at different temperatures. One example described the effect of the hard and soft coronas on the emission intensity of magnetic NPs functionalized with an Eu^{3+} complex. Eu^{3+} ions present certain electric dipole transitions that are sensitive to the electromagnetic local symmetry, and thus their light emission can be used to extract information about it, including atom bond distances.[65] These findings suggest a distortion in the local point symmetry upon addition of different concentrations of blood plasma to the sample, supporting an increased interaction with plasma proteins. Also important is the fact that the biocorona may yield autofluorescence and light absorption bands that potentially interact with luminescent probes, causing energy transfer processes especially in the visible range.

Another excellent example is the effect of the environmental refractive index on the lifetime of optical nanosensors. Experimental lifetime, τ_{exp}, which is the parameter measured in lifetime-based thermometry, as given by equation (2), includes radiative and a non-radiative contributions. Focusing on the radiative lifetime ($\tau_r=1/k_r$), described as early as 1926, Perrin wrote for the first time an expression for τ_r stating that it depends on the refractive index,[66] as does k_r. The question then arises, how can the refractive index be defined? If we take again the example of dopants in a crystal host, the refractive index of a bulk material would be that of the crystal host. However, when the material is reduced in size and becomes smaller than the wavelength of light, this assumption is no longer accurate. Indeed, a definition has been proposed for an effective refractive index that takes into consideration the indexes of both the host and the solvent.[67, 68] This effective index depends on a filling factor, x, which represents how big the nanoparticle is, compared to the wavelength of light:

$$n_{eff} = x \cdot n_h + (1 - x) \cdot n_{sol} \qquad (5)$$

where n_{eff}, n_h and n_{sol} are the effective refractive index, the index of the host, and the index of the solvent, respectively. Illustrative examples have been provided by Meijerink and co-workers, using 4 nm diameter $LaPO_4:Ce^{3+}$ nanocrystals to demonstrate that a variation of the solvent refractive index from 1.36 to 1.48 triggers a ≈ 26% change in Ce^{3+} lifetime (from 35 to 26 ns).[69] Similar results were obtained in 4 nm diameter $LaPO_4:Tb^{3+}$ nanoparticles coated by a 1 nm thick undoped shell. The shell was shown to have a negligible effect on the refractive index, because its thickness was too

small compared to the wavelength. It was however beneficial to increase the luminescence intensity, as it provided a separation between emitting ions in the particle (Tb^{3+}) and molecules in the solvent that could otherwise non-radiatively act as quenchers through their vibrational modes (vibrational modes of C-H and N-H bonds, mainly). Indeed, the luminescence quantum yield was shown to improve in ≈ 13% in the presence of the coating shell.

In a different example, based on the same type of NPs co-doped with Ce^{3+} and Tb^{3+}, the same group demonstrated that the efficiency of energy transfer between both ions decreased as the external refractive index increased. In this material, Ce^{3+} could absorb the excitation energy, and then transfer it to Tb^{3+}, which acted as the emitter. When changing the solvent refractive index, the emission rate of Ce^{3+} also changed, affecting the energy transfer efficiency and ultimately the emission from Tb^{3+}.[70] In these examples, we have seen the consequences of environmental changes on the luminescence emission from metal ions within a crystal. These conclusions can also be extended to other types of fluorophores, but the extent of the resulting effect will be different for each specific case. For instance, in some organic molecules such as GFP, lifetime is so sensitive to the surrounding refractive index that it becomes a suitable technique to measure its value in organelles inside cells.[71,72] Using this and other techniques, it has been determined that the refractive index within a cell varies with protein concentration, salt concentration and, to a lower extent, with temperature. Still, typical refractive index values range from 1.355-1.365 for the nucleus, 1.400-1.420 for the mitochondria, 1.46 for the plasma membrane, and around 1.60 for lysosomes.[71–74] If we instead consider *in vivo* situations in which whole tissues or organs are to be studied, the same range of refractive indexes can be identified when comparing different locations in bones, skin, eyes, etc.[75] According to the above referred studies under controlled conditions, it is clear that the optical properties of a thermal LNM probe may vary (even significantly) at different locations within a cell or tissue. The medium refractive index should be known prior to devising a specific thermometry experiment, to avoid inaccurate thermal readings. Indeed, the three parameters described above regarding the effect of refractive index (lifetime, intensity and energy transfer) also depend on temperature, and have been proposed for nanothermometry.

With this information at hand, the practical use of LNMs in heterogeneous environments may seem unlikely. However, understanding the problem is the basis on top of which accurate nanothermometers can be developed. Indeed, some good examples have been reported that pave the way towards practical sensors. Naturally, the proposed sensors should first be tested, to check the extent to which environmental effects may interfere with thermal readings. Indeed, in some reported examples the effect of the microenvironment appears to be negligible (or at least within measurement error). This was shown by Hayashi et al.,[2] using a thermoresponsive polymer whose emission lifetime changed with temperature. A series of careful control experiments showed that the LNM lifetime did not depend on pH or viscosity, but slightly changed with ionic strength. As the nanothermometers were designed for intracellular thermometry, ionic strength might compromise the accuracy of the thermal reading. To solve this problem, a control experiment was performed using another polymer with negligible thermal sensitivity, but with the same dependence of lifetime on ionic strength as that of the LNM. Introducing both polymers into HeLa cells, it was possible to map the fluorescence lifetime internally (**Figure 9b**) and, from a comparison of both samples, thermal information was derived, ensuring that ionic strength was not affecting the readout. In this way, a ≈ 1 ºC thermal difference between nucleus and cytoplasm was determined.

Towards accurate thermal measurements. When a new material is conceptually proposed for nanothermometry, a complete thermal calibration must be performed under a well-defined state, typically as a dry powder or as a colloidal dispersion. However, when the targeted applications involve complex biological environments, more extensive calibration may be required. Aiming to clarify what a complete characterization would be, a set of steps for a standard protocol have been proposed,[11] specifically focusing on biomedical applications. When dealing with LNMs destined for *in vitro* studies, the two main identified parameters are pH and dynamic viscosity, in particular focusing on a pH range of 6.0 - 7.5, and viscosity range of 1×10^{-3} - 20 Pa.s. The situation is more complex for *in vivo* studies because LNM concentration and aggregation are difficult to control. It is therefore advised to perform an *ex vivo* calibration in extracted organs relevant to the expected biodistribution.

Although the tested nanothermometers may appear to be accurate, a good strategy to ensure correct thermal readings comprises including an additional nanothermometer control material within the same experiment. This test is particularly interesting if the selected thermal probe is based on a different luminescence temperature measurement strategy, so that environmental changes are unlikely to equally interfere with both mechanisms. Interference of environmental conditions other than temperature would then lead to a disagreement between both probes, which can be readily detected. This strategy has been used in intracellular studies analysing thermogenesis in brown adipocytes.[28] In this work, one of the probes was based on a thermoresponsive polymer and its fluorescence lifetime,[21] whereas a second thermometer was based on the emission intensity of a hydrophilic gel that would collapse upon heating, expelling water molecules and thereby enhancing the emission of a fluorophore inside.[76] The combination of these two temperature measurement strategies is particularly relevant for *in vivo* experiments where many environmental factors may interfere with the thermal reading.[11] One practical requirement is that both luminescence signals can be easily differentiated. In the previous example, both polymers can be excited at around 450 nm and present an emission band ranging from 500 to 700 nm, with a maximum at *ca*. 560 nm. Since there is a significant overlap in the emission properties of both polymers, ideally two separate experiments should be performed to achieve maximum thermal accuracy. Whilst feasible *in vitro*, using standard fluorescence microscopes programmed to do sequential

imaging in a short time frame, this is not practical *in vivo*, under diagnostic and/or therapeutic situations. Hence, both thermal probes should display clearly differentiated luminescent properties that allow simultaneous measurements of both LNM emissions.[77]

It is thus clear that both careful experimental design and a complete calibration are needed, and rationally adapted to each proposed application. However, these tasks may become simpler if nanothermometers are specifically designed to minimize interferences from surrounding molecules with their optical properties. For instance, the distance between luminescent ions and a possible quencher is key to determine how likely the quenching effect would be noticed. Taking lanthanide-based luminescence as an example, the influence of surrounding molecules on doped nanoparticles is typically lower than it would be on lanthanide-based organic complexes, in which the luminescent ion is less isolated.[68] For the same reason, NP size also plays a role because in larger particles the dopants are farther away from the surrounding environment. Another size-related effect can be derived from the definition of the effective refractive index, as shown in equation (5), as larger particles will be closer in size to the illumination wavelength and thus scatter light more efficiently. A suitable alternative to making larger nanoparticles may be the encapsulation within (polymeric) micelles or growing a non-luminescent inorganic shell. In the case of luminescent NPs such as QDs, growth of a non-luminescent inorganic shell is the preferred option because core particle size largely determines the emission wavelength of the QD. In the case of lanthanide-doped NPs, a coating shell would also be efficient, as quenching paths to external molecules are interrupted, an approach that might be beneficial to keep size to a minimum.

Conclusion and perspectives

Precise monitoring of temperature is critical toward understanding many naturally occurring biological processes, ultimately aiming at the diagnosis and treatment of various pathophysiological disease states, and even to improve current cryopreservation techniques. Regardless of the final application for temperature determination at the cell, tissue, or organ level, the use of non-invasive methods is of crucial importance. Luminescent nanomaterials are proposed as the optimum choice. These materials feature temperature-dependent photoluminescence, with tailored excitation and emission in the biological windows. As such, the interactions between the photoluminescent properties of LNMs and the absorbing and scattering properties of biological tissue are minimized. However, both the excitation beam and emitted light interact with tissue in ways that must be understood and considered to accurately measure temperature.

If we focus on the effects of a biological environment on the excitation beam, optimization of beam width can be an asset because lateral scattering may contribute to reach deeper tissue. Also, optimization of the final thermal reading requires a good knowledge of autofluorescence within the biological windows. With the development of biomedical techniques exploiting these wavelength ranges, it has been discovered that some components such as melanin or animal food are luminescent in the NIR. It would not be surprising, that, during coming years, other biological components are also found to emit, but it can be expected that this autofluorescence will be lower than that in the visible.

If we focus instead on the interaction of emitted light with tissue, the major problem to resolve is the deformation of luminescence spectra due to the absorption by tissue, which is a relevant source of error when absolute temperature is to be measured. For this reason, most examples in which temperature has been measured *in vivo* evaluate transient rather than absolute temperature. Some recalibration solutions have been proposed to circumvent this problem, which occurs mainly in LNMs based on rare-earth doped nanoparticles with thermalized energy states. Additional solutions will arise through the development of materials with a thermalized ground level in which recalibration is not needed because the intensity ratio is built from the same emission band, excited at two different wavelengths. However, these options are based on lanthanide-doped materials, typically with a low emission intensity compared to other fluorophores. This is a major limiting factor regarding penetration depth and thermal resolution, and thus more efficient emitters are desired for in depth applications. Regarding lanthanides, strategies based on the use of optical antennas to better absorb the excitation light have been proposed, but to our knowledge not yet implemented in (bio)applications. An alternative path may involve LNMs doped with transition metals, but so far they have not reached the performance of lanthanide-doped materials, especially in the thermal range of interest in biology.

Given the increasing awareness of the problems arising from the interaction of light with tissue, new measurement strategies will likely arise, aiming for better thermometry performance with simpler experimental setups that can be implemented in biology labs or in clinical settings. Improvement of penetration depth or thermal resolution to measure absolute temperature may be achieved with lifetime-based thermometers, as they are not affected by spectral distortions. However, a complete characterization of the material and its luminescence in different environments will be key to ensure sufficient accuracy.

The relative sensitivity of most nanothermometers is often insufficient, at least when the variation of only one parameter is taken into account. Hence, methods have been developed to measure temperature via two luminescence emission characteristics simultaneously, e.g., peak position, band width, polarization anisotropy, etc., and then apply multiparameter linear regression for temperature determination. This can be carried out by using either two different probes or just one with multiple readout options, which is possible with Ag_2S nanoparticles. Given its high versatility and brightness, Ag_2S is one of the most promising materials towards practical *in vivo* applications, and particularly interesting synthesis strategies have been patented. Whereas multiparameter and multiprobe schemes improve the accuracy and reproducibility of LNMs for temperature sensing, it is paramount that the interactions between excitation and emission photons with the biological milieu be kept to a minimum, to avoid loss of signal intensity, and hence sensitivity, during the measurement. This multiparameter technique is also relevant if we consider the effect of the LNM's microenvironment on their

spectroscopic properties. To avoid measurement errors based on this interaction, standardization protocols aim to unveil any uncontrolled change on the luminescence that may trigger inaccuracies during thermal reading. However, since different luminescence characteristics depend differently on the microenvironment, the use of more than one emission parameter, or more than one LNM probe, appears as a promising strategy to identify unexpected effects. Alternatively, the design of thermal probes protected from the microenvironment, e.g. by encapsulation, may be an optimal strategy in some scenarios. However, for hyperthermia treatments in particular, the stability of such encapsulations at different temperatures must be tested, in addition to the effect of the biocorona.

In non-clinical settings, one method to reduce the interfering properties of complex biological tissue is to simplify the biological model, i.e., moving from *in vivo* studies involving multi-organ systems, to *in vitro* organ-on-a-chip devices or spheroids. Our understanding of the natural or controlled formation (i.e., additive manufacturing) of *in vitro* tissue and organ models has vastly improved, allowing reproducible and realistic pre-*in vivo* studies. Thanks to their controllable physiological and biochemical traits, 3D biological models, combined with LNMs, will play an important role in furthering our understanding of hyperthermia. That said, when writing this tutorial review, we discovered a considerable lack of data relating to the use of LNMs for temperature sensing in 3D cell models such as spheroids, organoids, and organ-on-a-chip devices. We propose that these models will be of special importance to better understand the temperature sensing abilities of LNMs, prior *in vivo* investigation. Issues such as the uncontrolled LNM aggregation as a result of *i.e.* biocorona formation, or a reduced luminescence readout due to light attenuation across tissue interfaces, can be studied with *in vitro* 3D models, thereby adhering to the 3R´s of Replacement, Reduction, and Refinement.

Conflicts of interest

There are no conflicts to declare.

Acknowledgements

L. M. L.-M. acknowledges funding from the European Research Council (ERC Advanced Grant 787510, 4DBIOSERS) and MCIN/AEI /10.13039/501100011033 (grant # Maria de Maeztu Unit of Excellence No. MDM-2017-0720). M.Q. acknowledges funding from MCIN/AEI /10.13039/501100011033 (grant # PID2019-110632RB-I00).

References

1 P. Gas, *Przeglad Elektrotechniczny,* 2011, **87** (12b) 37-40.

2 A. R. Rastinehad, H. Anastos, E. Wajswol, J. S. Winoker, J. P. Sfakianos, S. K. Doppalapudi, M. R. Carrick, C. J. Knauer, B. Taouli, S. C. Lewis, A. K. Tewari, J. A. Schwartz, S. E. Canfield, A. K. George, J. L. West and N. J. Halas, *Proc. Natl. Acad. Sci.*, 2019, **116**, 18590–18596.

3 A. Lozano and F. Hassanipour, *Infrared Phys. Tech.*, 2019, **97**, 244–257.

4 A. Lozano, J. C. Hayes, L. M. Compton, J. Azarnoosh and F. Hassanipour, *Sci. Rep.*, 2020, **10**, 10105.

5 R. R. Anderson and J. A. Parrish. *J. Invest. Dermatol.*, 1981, **77**, 13-19.

6 E. Doruk Onal and Kaan Guven, *J. Phys. Chem. C*, 2017 **121**, 684-690.

7 A. Nexha, J. J. Carvajal, M. C. Pujol, F. Díaz and M. Aguiló, *Nanoscale*, 2021, **13**, 7913–7987.

8 M. Quintanilla and L. M. Liz-Marzán, *Nano Today*, 2018, **19**, 126–145.

9 D. Jaque and F. Vetrone, *Nanoscale*, 2012, **4**, 4301–4326.

10 J. Zhou, B. del Rosal, D. Jaque, S. Uchiyama and D. Jin, *Nat. Methods.*, 2020, **17**, 967–980.

11 A. Bednarkiewicz, L. Marciniak, L. D. Carlos and D. Jaque, *Nanoscale*, 2020, **12**, 14405-14421.

12 H. Peng, H. Song, B. Chen, J. Wang, S. Lu, X. Kong and J. Zhang, *J. Chem. Phys.*, 2003, **118**, 3277–3282.

13 Y. Shen, H. D. A. Santos, E. C. Ximendes, J. Lifante, A. Sanz-Portilla, L. Monge, N. Fernández, I. Chaves-Coira, C. Jacinto, C. D. S. Brites, L. D. Carlos, A. Benayas, M. C. Iglesias-de la Cruz and D. Jaque, *Adv. Funct. Mater.*, 2020, **30**, 2002730.

14 G. Kucsko, P. C. Maurer, N. Y. Yao, M. Kubo, H. J. Noh, P.K. Lo, H. Park and M. D. Lukin, *Nature,* 2013, **500**, 54–58.

15 E. Maturi, C. D. S. Brites, E. C. Ximendes, C. Mills, B. Olsen, D. Jaque, S. J. L. Ribeiro and L. D. Carlos, *Laser Photonics Rev.*, 2021, 2100301.

16 Y. Cheng, Y. Gao, H. Lin, F. Huang and Y. Wang, *J Mater. Chem. C*, 2018, **6**, 7462–7478.

17 K. Trejgis, R. Lisiecki, A. Bednarkiewicz and L. Marciniak, *J. Lumin.,* 2020, **224**, 117295.

18 J. S. Donner, S. A. Thompson, C. Alonso-Ortega, J. Morales, L. G. Rico, S. I. C. O. Santos and R. Quidant, *ACS Nano*, 2013, **7**, 8666–8672.

19 S. A. Thompson, I. A. Martínez, P. Haro-González, A. P. Adam, D. Jaque, J. B. Nieder and R. de la Rica, *ACS Photonics*, 2018, **5**, 2676–2681.

20 M. D. Dramicanin, *J. Appl. Phys.,* 2020, **128**, 040902

21 T. Hayashi, N. Fukuda, S. Uchiyama and N. Inada, *PLOS ONE*, 2015, **10**, e0117677.

22 H. D. A. Santos, D. Ruiz, G. Lifante, C. Jacinto, B. H. Juarez and D. Jaque, *Nanoscale*, 2017, **9**, 2505–2513.

23 M. Nakano, Y. Arai, I. Kotera, K. Okabe, Y. Kamei and T. Nagai, *PLOS ONE*, 2017, **12**, e0172344.

24 G. Baffou, H. Rigneault, D. Marguet and L. Jullien, *Nat. Methods*, 2015, **12**, 803.

25 Y. Takei, S. Arai, A. Murata, M. Takabayashi, K. Oyama, S. Ishiwata, S. Takeoka and M. Suzuki, *ACS Nano*, 2014, **8**, 198–206.

26 M. Suzuki, V. Zeeb, S. Arai, K. Oyama and S. Ishiwata, *Nat. Methods*, 2015, **12**, 802–803.

27 M. C. Rajagopal and S. Sinha, *Cell Biochem. Biophys.*, 2021, **79**, 359–373.

28 H. Kato, K. Okabe, M. Miyake, K. Hattori, T. Fukaya, K. Tanimoto, S. Beini, M. Mizuguchi, S. Torii, S. Arakawa, M. Ono, Y. Saito, T. Sugiyama, T. Funatsu, K. Sato, S. Shimizu, S. Oyadomari, H. Ichijo, H. Kadowaki and H. Nishitoh, *Life Sci. Alliance*, 2020, **3**, e201900576.

29 M. Zanoni, F. Piccinini, C. Arienti, A. Zamagni, S. Santi, R. Polico, A. Bevilacqua and A. Tesei, *Sci. Rep.*, 2016, **6**, 19103.

30 C. Egloff-Juras, I. Yakavets, V. Scherrer, A. Francois, L. Bezdetnaya, H.-P. Lassalle and G. Dolivet, *Int. J. Molec. Sci.*, 2021, **22**, 1966.

31 B. McCarthy, A. Cudykier, R. Singh, N. Levi-Polyachenko and S. Soker, *Sci. Rep.*, 2021, **11**, 1532.

32 M. Quintanilla, I. García, I. de Lázaro, R. García-Alvarez, M. Henriksen-Lacey, S. Vranic, K. Kostarelos and L. M. Liz-Marzán, *Theranostics*, 2019, **9**, 7298-7312.

33 PerkinElmer, Identity Verification and Quality Testing of Polymers Using Mid Infrared Spectroscopy, *Azo Materials,* 2015, https://www.azom.com/article.aspx?ArticleID=12386

34 M. Z. Vardaki and N. Kourkoumelis, *Biomed. Eng. Comput. Biol.*, 2020, **11**, 1-15.

35 NIH, Rodent Injection Routes, https://oacu.oir.nih.gov/system/files/media/file/2021-02/rodentinjection.pdf

36 S. S. Laha, A. R. Naik, E. R. Kuhn, M. Alvarez, A. Sujkowski, R. J. Wessells and B. P. Jena, *Nano Lett.*, 2017, **17**, 1262–1268.

37 E. C. Ximendes, U. Rocha, B. del Rosal, A. Vaquero, F. Sanz-Rodríguez, L. Monge, F. Ren, F. Vetrone, D. Ma, J. García-Solé, C. Jacinto, D. Jaque and N. Fernández, *Avd. Health. Mater.*, 2016, **6**, 1601195.

38 H. D. A. Santos, E. C. Ximendes, M. del C. I. la Cruz, I. Chaves-Coira, B. del Rosal, C. Jacinto, L. Monge, I. Rubia-Rodríguez, D. Ortega, S. Mateos, J. GarcíaSolé, D. Jaque and N. Fernández, *Adv. Funct. Mater.*, 2018, **28**, 1803924.

39 B. del Rosal, D. Ruiz, I. Chaves-Coira, B. H. Juárez, L. Monge, G. Hong, N. Fernández and D. Jaque, *Adv. Funct. Mater.*, 2018, **28**, 1806088.

40 K. Khosla, Y. Wang, M. Hagedorn, Z. Qin and J. Bischof, *ACS Nano*, 2017, **11**, 7869–7878.

41 N. Manuchehrabadi, Z. Gao, J. Zhang, H. L. Ring, Q. Shao, F. Liu, M. McDermott, A. Fok, Y. Rabin, K. G. M. Brockbank, M. Garwood, C. L. Haynes and J. C. Bischof, *Sci. Transl. Med.*, 2017, **9**, eaah4586.

42 Z. Qin and J. C. Bischof, *Chem. Soc. Rev.*, 2012, **41**, 1191–1217.

43 F. W. Kleinhans, S. Seki and P. Mazur, *Cryobiology*, 2010, **61**, 231–233.

44 M. Henriksen-Lacey, S. Carregal-Romero and L. M. Liz-Marzán, *Bioconjugate Chem.*, 2017, **28**, 212–221.

45 A. Vogel and V. Venugopalan, *Chem. Rev.* 2003, **103**, 577–644.

46 Y. Shen, J. Lifante, I. Z. Gutierrez, M. Fuente-Fernández, M. Granado, N. Fernández, J. Rubio-Retama, D. Jaque, R. Marin, E. Ximendes and A. Benayas, *Adv. Mater.*, 2021, **34**, 2107764

47 Z. Gajinov, M. Matić, S. Prćić and V. Đuran, *Serbian J. Dermatol. Venerol.*, 2010, **2**, 131–136.

48 J. F. Algorri, M. Ochoa, P. Roldán-Varona, L. Rodríguez-Cobo and J. M. López-Higuera, *Cancers*, 2021, **13**, 3484.

49 S. L. Jacques, *Phys. Med. Biol.*, 2013, **58**, R37-61

50 Guidelines from International Commission on Non-Ionizing Radiation Protection (ICNIRP) regarding NIR radiation https://www.icnirp.org/en/frequencies/infrared/index.html

51 S. Bhaumik, J. DePuy and J. Klimash, *Lab Animal*, 2007, **36**, 40–43.

52 J. Lifante, Y. Shen, E. Ximendes, E. Martín Rodríguez and D. H. Ortgies, *J. App. Phys.*, 2020, **128**, 171101.

53 E. Hemmer, N. Venkatachalam, H. Hyodo, A. Hattori, Y. Ebina, H. Kishimoto and K. Soga, *Nanoscale*, 2013, **5**, 11339–11361.

54 R. Richards-Kortum and E. Sevick-Muraca, *Annu. Rev. Phys. Chem.*, 1996, **47**, 555–606.

55 A. N. Bashkatov, E. A. Genina, V. I. Kochubey and V. V. Tuchin, *J. Phys. D: Appl Phys*, 2005, **38**, 2543–2555.

56 C. Ash, M. Dubec, K. Donne and T. Bashford, *Lasers Med. Sci.*, 2017, **32**, 1909–1918.

57 Y. Shen, J. Lifante, N. Fernández, D. Jaque and E. Ximendes, *ACS nano*, 2020, **14**, 4122–4133.

58 V. K. Nagarajan, V. R. Gogineni, S. B. White and B. Yu, *Int. J. Hyperthermia*, 2018, **35**, 1–7.

59 J. Lifante, Y. Shen, I. Z. Gutierrez, I. Rubia-Rodríguez, D. Ortega, N. Fernandez, S. Melle, M. Granado, J. Rubio-Retama, D. Jaque and E. Ximendes, *Adv. Sci.*, 2021, **8**, 2003838.

60 M. Quintanilla, Y. Zhang and L. M. Liz-Marzán, *Chem. Mater.*, 2018, **30**, 8, 2819–2828.

61 M. D. Shinn, W. A. Sibley, M. G. Drexhage and R. N. Brown, *Phys. Rev. B,* 1983, **27**, 6635.

62 S. Balabhadra, M. L. Debasu, C. D. S. Brites, R. A. S. Ferreira and L. D. Carlos, *J. Phys. Chem. C*, 2017, **121**, 13962–13968.

63 M. L. Debasu, D. Ananias, I. Pastoriza-Santos, L. M. Liz-Marzán, J. Rocha and L. D. Carlos, *Adv. Mater.*, 2013, **25**, 4868–4874.

64 A. Skripka, A. Benayas, D. S. Brites, I R. Martín, L D. Carlos, and F Vetrone, *Nano Letters*, 2020, **20**, 7648-7654.

65 L. U. Khan, R. Petry, A. J. Paula, M. Knobel, and D. S. T. Martinez, *ChemNanoMat.,* 2018, **4**, 1202-1208.

66 F. Perrin, *J. Phys. Radium*, 1926, **7**, 390–401.

67 D. Toptygin, *J. Fluorescence*, 2003, **13**, 201–219.

68 R. S. Meltzer, S. P. Feofilov, B. Tissue and H. B. Yuan, *Phys. Rev. B*, 1999, **60**, R14012–R14015.

69 T. Senden, F. T. Rabouw and A. Meijerink, *ACS Nano*, 2015, **9**, 1801–1808.

70 F. T. Rabouw, S. A. den Hartog, T. Senden and A. Meijerink, *Nat. Commun.*, 2014, **5**, 3610.

71 H.-J. van Manen, P. Verkuijlen, P. Wittendorp, V. Subramaniam, T. K. van den Berg, D. Roos and C. Otto, *Biophys. J.*, 2008, **94**, L67–L69.
72 C. L. Tregidgo, J. A. Levitt and K. Suhling, *J. Biomed. Opt.*, 2008, **13**, 031218.1–031218.8.
73 A. Pliss and P. N. Prasad, *Meth. Appl. Fluorescence*, 2020, **8**, 032001.
74 P. Y. Liu, L. K. Chin, W. Ser, H. F. Chen, C.-M. Hsieh, C.-H. Lee, K.-B. Sung, T. C. Ayi, P. H. Yap, B. Liedberg, K. Wang, T. Bourouina and Y. Leprince-Wang, *Lab Chip*, 2016, **16**, 634–644.
75 R. Khan, B. Gul, S. Khan, H. Nisar and I. Ahmad, *Photodiagnosis Photodyn. Ther.*, 2021, **33**, 102192.
76 C. Gota, K. Okabe, T. Funatsu, Y. Harada and S. Uchiyama, *J. Am. Chem. Soc.*, 2009, **131**, 2766–2767.
77 X. Lin, M. Kong, N. Wu, Y. Gu, X. Qiu, X. Chen, Z. Li, W. Feng and F. Li, *ACS Appl. Mater. Interfaces*, 2020, **12**, 52393–52401.